

A Follow-up Investigation into the Recharge Pathways and Mechanisms in the Northern Segment of the Edwards Aquifer, Bell County, Texas



A research report submitted to the Clearwater Underground Water Conservation District, Bell County, Texas

Final Report, December 2016

Submitted By:

Stephanie S. Wong, graduate student

Dr. Joe C. Yelderman Jr., Ph.D., P.G.

Baylor University, Department of Geosciences



Executive Summary

Efforts to learn more about the hydrologic processes in the Northern Segment of the Edwards Balcones Fault Zone aquifer, specifically in the Salado Springs complex, revealed several important discoveries that will aid water management and direct future research needs. These discoveries are listed below with interpretations regarding their potential significance.

1. Progress using LiDAR data to detect recharge features has been difficult and time consuming but is progressing slowly. A work-flow for identifying potential karst features using a mixture of manual and semi-automatic processes has been developed for the study area. The LiDAR data still look promising for determining areas of important recharge potential. Some potential fractures have been identified for further analysis.
2. Data collected with a multi-parameter datalogger in the Stagecoach Inn Cave well indicated rapid groundwater responses to large rainfall events. The data also show slight water quality changes. The responses to recharge captured by the datalogger provide important timing information to aid in the development of future monitoring strategies.
 - a. Nitrogen data from field and laboratory analysis showed values that are interpreted to be slightly above expected background levels but no nitrate values were observed to be over the drinking water limit.
 - b. The nitrogen data warrant further investigation and monitoring.
3. Data collected with a Solinst hand-held meter along cross-sections of Salado Creek and adjacent springs show patterns helpful in understanding groundwater/surface-water interactions and potential areas of salamander habitat.
 - a. Specific conductance (SC) and temperature (T) measurements in cross sections of Big Boiling Spring as well as upstream and downstream of the confluence between Big Boiling Spring discharge and Salado Creek confirm the mixing patterns of groundwater and surface water from Big Boiling Spring.
 - b. The cross section data are important to quantify groundwater/surface water mixing, aid in habitat assessments, and aid in water sample location selection.
4. Thermography using a handheld FLIR camera has helped delineate potential salamander habitat in the springs and spring runs at several springs. The thermography also has better delineated the exact areas of groundwater interaction with surface water and confirmed previous cross section studies.
5. Spring Inventory protocol (SIP) and Spring Ecosystem Assessment Protocol (SEAP) were used to categorize the springs in the downtown area with internationally published protocols for comparisons of baseline and possibly future management conditions.

Contents

Executive Summary	i
Contents	ii
List of Figures	iii
Project Overview	1
- Project area	
Recharge features characterization.....	3
Groundwater monitoring.....	7
- Multi-parameter monitoring	
- Multi-parameter monitoring data	
- Nitrate monitoring	
Groundwater – surface water interaction.....	15
- Stream profiling	
- Thermography (FLIR)	
Springs assessment.....	25
- SIP and SEAP	
Summary & Project Conclusions	30
Recommendations	31
References	32
Appendices	33
- Appendix A: Dissolved nitrate /nitrite concentrations for Salado Springs	
- Appendix B: Springs Assessment: SIP and SEAP datasheets	
- Appendix C: Sunpath diagrams for Salado Springs	

List of Figures

Figure 1. This study was conducted in Northern Segment of the Edwards Balcones Fault Zone aquifer in Bell County (modified from Jones, 2003).....	2
Figure 2. Location of springs in the Salado Springs complex.....	2
Figure 3. Overview of LiDAR data collection to produce elevation surfaces which can then be used for analysis.....	3
Figure 4. Overview of workflow for identifying karst features using LiDAR data.....	4
Figure 5. Map of depressions at Robertson Ranch.....	5
Figure 6. Aspect map of Robertson Ranch, with manually-determined lineations.....	5
Figure 7. Rose diagram plotted using GeoRose 0.5.1.....	6
Figure 8. A major lineation extrapolated from Robertson Ranch matches the field-determined orientation of a lineation observed at Big Boiling springs.....	6
Figure 9. A multi-parameter datalogger has been deployed in the Stagecoach Inn cave well since May 2013 to collect data on water level, temperature, and specific conductance.....	7
Figure 10. Hydrologic conditions at the Stagecoach Inn cave well from June 2013 to September 2016.....	9
Figure 11. Hydrologic conditions at the Stagecoach Inn cave well in May 2015.....	10
Figure 12. Nitrate trend data collected by the Troll 9500 sonde from October 7 to November 30, 2015 at the Stagecoach Inn Cave well.....	11
Figure 13. Map of nitrate sampling locations around downtown Salado.....	12
Figure 14. Nitrate concentrations at Salado Springs over the Labor Day long weekend.....	13
Figure 15. Nitrate trend data collected by the Troll 9500 sonde and grab samples from September 1-21, 2016 at the Stagecoach Inn Cave well.....	14
Figure 16. Diagram of downtown Salado Creek showing key features.....	15
Figure 17. Discharge, specific conductance and temperature measurements at cross-section 1, located in the spring flow of Big Boiling Spring.....	16
Figure 18. Discharge, specific conductance and temperature measurements at cross-section 2, located in the natural channel of Salado Creek.....	17
Figure 19. Discharge, specific conductance and temperature measurements at cross-section 3, located in the natural channel of Salado Creek, downstream of the confluence with Big Boiling Spring.....	18
Figure 20. Abrupt contrast between clear groundwater flowing from Big Boiling Springs and sediment-laden surface water in Salado Creek after a small rainfall and during low spring flow conditions.....	20
Figure 21. No contrast between clear groundwater flowing from Big Boiling Springs into clear baseflow in Salado Creek.....	20
Figure 22. FLIR E63900 handheld infrared camera.....	23
Figure 23. Side Spring looking northward from the south bank of Salado Creek in downtown Salado, Texas.....	23
Figure 24. Temperature profiles in Salado creek and Big Boiling Spring, April 6, 2016.....	22
Figure 25. Specific conductance profile at section 3 April 6, 2016.....	22
Figure 26. FLIR infrared image of profile Section 3 downstream from Big Boiling Spring showing the warmer temperatures associated with the groundwater discharge of Big Boiling Spring along the REW edge of the creek.....	23

Figure 27. <i>Ludwigia</i> growing near the REW bank of Salado Creek downstream from the spring discharge of Big Boiling Spring, April 6, 2016.....	23
Figure 28. Rheocrene spring (Springer and Stevens, 2009).....	26
Figure 29. Limnocrene spring (Springer and Stevens, 2009).....	26
Figure 30. The Solar Pathfinder™	27
Figure 31. Robertson Spring has characteristics of both a rheocrene spring as well as a limnocrene spring.....	27
Figure 32. Big Boiling Spring has characteristics of a rheocrene spring and a limnocrene spring.....	28
Figure 33. Little Bubbly Spring is best classified as a rheocrene spring.....	28
Figure 34. Side Spring is best classified as a rheocrene spring.....	28
Figure 35. Critchfield Spring has characteristics of both a limnocrene spring as well as a rheocrene spring.....	29
Figure 36. Doc Benedict Spring is best classified as a limnocrene spring.....	29
Figure 37. Anderson Spring is best classified as a limnocrene spring.....	29

Project Overview

A body of research was undertaken by Baylor University (“Baylor”), in collaboration with the Clearwater Underground Water Conservation District (CUWCD), to gain a deeper understanding of the Northern Segment of the Edwards Balcones Fault Zone (BFZ) Aquifer (the Northern Segment) for the purposes of providing insight for groundwater resource management and supporting collaboration between the district and community stakeholders. Phase 1 of this research began in 2013 and focused on instrumentation, field tests, and feasibility studies to help build knowledge of how much recharge occurs and the pathways that recharge takes to the aquifer. Over the course of phase 1 research, Baylor and CUWCD realized that further efforts were necessary to continue data collection and interpretation. Phase 2 research, which spanned spring and summer 2016, focused on continuing monitoring activities while adding new monitoring parameters, refining field tests and samples, as well as analysis and interpretation of data gathered during phase 1 research. After a brief description of the study area, this report is divided into sections regarding recharge features characterization, groundwater monitoring, groundwater-surface water interaction, and springs assessment. Each section describes the rationale for a given work, methods and instrumentation employed, and results.

Although this report serves as a final summary of the research efforts completed under the 2016 contract between Baylor and CUWCD, there is still much to learn about the Northern Segment system. Collaborative efforts, monitoring, and data gathering are on-going.

Project area

This body of research was conducted in the outcrop portion of the Northern Segment in Bell County (Figure 1). Focus was placed on the Salado Springs complex in downtown Salado due to their importance as critical habitat for the Salado salamander, their use as a measure of the CUWCD’s DFC, and ease of access (Figure 2).

There are three formations that comprise the Northern Segment of the Edwards Balcones Fault Zone aquifer. They are in ascending order: the Comanche Peak Formation, the Edwards Formation and the Georgetown Formation. All of these units are sedimentary rocks, Cretaceous in age, and comprised mainly of carbonate (limestones). The Edwards and Comanche Peak formations are part of the Fredricksburg Group and the Georgetown is part of the Washita Group. They are fairly well connected hydraulically and considered as one hydrostratigraphic unit referred to as the Edwards aquifer; specifically the Northern Segment of the Edwards Balcones Fault Zone aquifer. The underlying confining unit is the uppermost member of the Walnut formation, the Keys Valley Marl, which is a carbonaceous clay. The overlying confining unit is the Del Rio Formation, a carbonaceous clay-rich unit that is often referred to as the Del Rio Clay (sometimes referred to as the Grayson Formation). Upper Cretaceous units overlying the Del Rio Formation and cropping out in the Salado Creek basin include the Buda Formation, Eagle Ford Group and the Austin Chalk. None of these are considered aquifers in this area. (Jones, 2003)

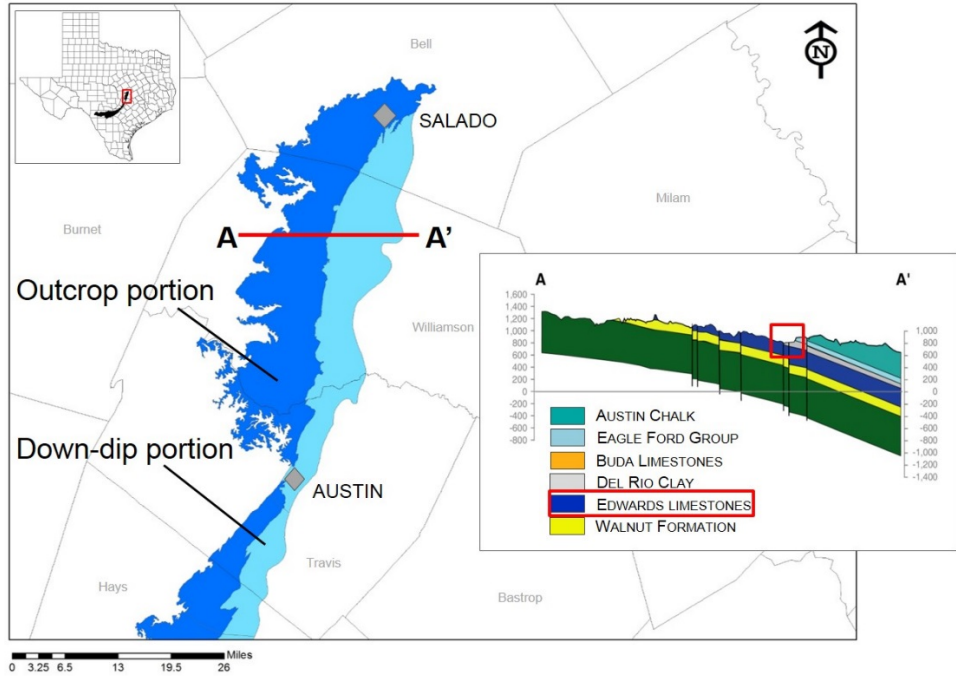


Figure 1. This study was conducted in Northern Segment of the Edwards Balcones Fault Zone aquifer in Bell County (modified from Jones, 2003).

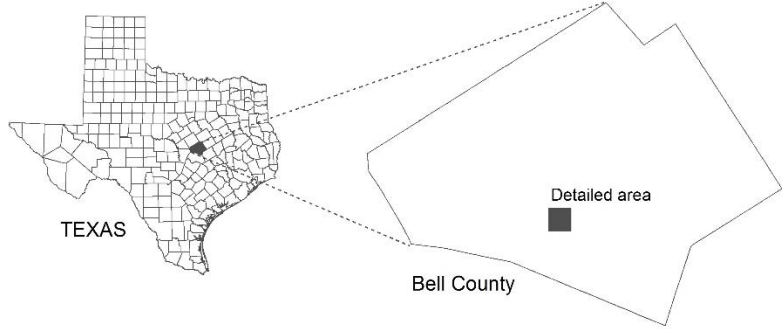


Figure 2. Location of springs in the Salado Springs complex, which was a focus area for this body of research due to ease of access and the springs' importance as a management parameter for CUWCD.

Recharge Features Characterization

Lidar

Lidar, which stands for *light detection and ranging*, is an active remote sensing technology that utilizes pulsed lasers to measure various properties of targets of interest. Lidar technology measures the relative distance between the scanning laser (air- or ground-based) and a target, and generates a point cloud representing the target surface (Figure 3-1; 3-2). Each point has an associated x, y, and z coordinate. Surfaces can be generated from the point cloud using interpolation methods, which can then be analyzed for karst features (Figure 3-3).

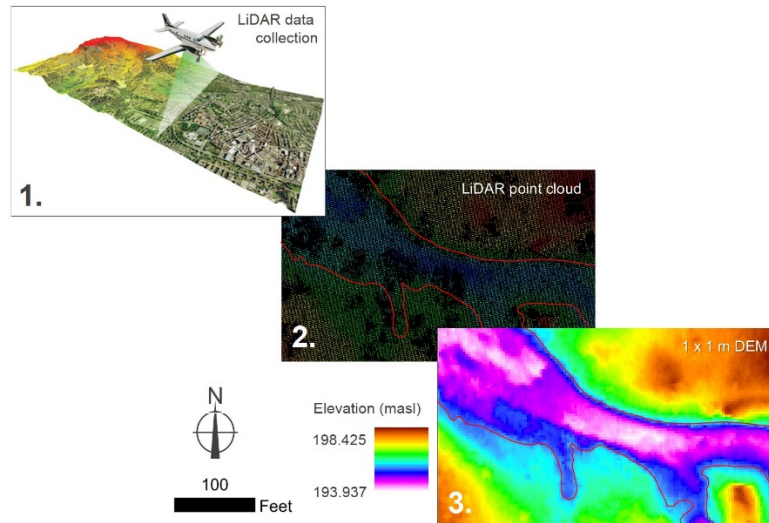


Figure 3. Overview of Lidar data collection to produce elevation surfaces which can then be used for analysis.

Approach

For this project, the original objectives were to: identify lineations and depressions using Lidar data, differentiate between geologic and anthropogenic lineations and depressions, and identify geologic lineations that are potential recharge features. Lidar data and 1 x 1 m DEMs were obtained from the Central Texas Council of Governments (CTCOG) in fall 2013. Bell County Lidar data were acquired through a partnership between CTCOG and TNRIS during spring of 2011. A Leica ALS50 phase II+ and a Leica ALS60 Lidar sensor (Gonzales Block) were used to collect multiple return data in the x, y, and z, dimensions; as well as intensity data (TNRIS, 2017). In our proof-of-concept exercise (phase 1), the workflow for identifying karst features involved manually isolating and extracting pixels that may indicate karst features, which were represented by pixels of lowest elevation. This process was slow due to the density of data generated by Lidar, and only very small areas could be dealt with at a time.

Through consultation with colleagues and published literature, separate workflows were developed to identify depressions and lineations that allowed dealing with more Lidar data at once (Figure 4). Both the depressions workflow and lineations workflow utilize ArcGIS capabilities and tools. To identify depressions, the 1 x 1 m DEM was first filled using the Fill tool. DEM datasets normally contain sinks which arise due to data resolution errors or rounding elevations to the nearest integer value (ESRI, 2017a). However in glacial or karst areas, data sinks may represent actual depressions in the landscape. Processing the DEM using the Fill tool created a continuous surface with no sinks. The original DEM and the filled DEM were subtracted from each other using the Raster Calculator, creating a difference surface. Pixels that were less than 1 m (3.28 ft) difference were filtered out since the spatial resolution of the Lidar DEM is 1 m. The surface after filtering represents depressions identified through this semi-

automatic workflow. A similar workflow was described by Gritzner (2006) to identify wetland depressions in Devils Lake Basin, North Dakota.

To identify lineations, a map of aspect was created from the original 1 x 1 m DEM. Aspect is the slope direction. The value of every cell in an aspect map is the maximum rate of change (or slope) for that cell relative to its neighbors, range from 0-360° as in a full circle (where 0° and 360° equal due north, 90° equals due east, 180° equals due south, and 270° equals due west), and indicates the compass direction that the surface faces at that location (ESRI, 2017b). Since most lineations in the area of interest are associated with the Balcones Fault Zone which runs NE-SW, developing an aspect map helped highlight lineations that were present. Additionally, aspect helped to differentiate geologic lineations which would mostly also be oriented NE-SW from anthropogenic lineations such as fence lines, unpaved paths, and roads. Lineations were identified and digitized manually. Comparison with aerial imagery aided in differentiating anthropogenic versus geologic lineations. Both depression and lineation workflows were applied to the Robertson Plantation property.

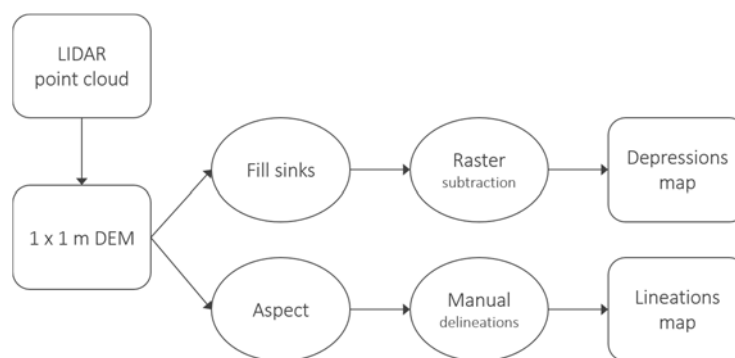


Figure 4. Overview of workflow for identifying karst features using LiDAR data. After a feasibility test in phase 1 research, separate workflows were developed to identify lineations and depressions.

Results and Discussion

The final depressions map is presented in Figure 5. Two main depression features are immediately apparent: the constructed pond towards the middle of the Robertson property, ranging from about 3 to 12 ft depth; and another depression near the eastern property line, ranging from about 3 to 9 ft depth. The spring run for Robertson Springs also shows up as a depression in the northeastern corner of the property.

The final lineations map is presented in Figure 6. Measured lineation orientation ranged from 4 – 359°, with an average orientation of 77°. When the orientations are summarized using a rose diagram (Figure 7), most lineations are oriented southwest-northeast, which agrees with the trend of the Balcones Fault Zone. The measured orientations also correlated with field observations. A lineation extending past the eastern property line was extrapolated to downtown Salado. By combining Lidar and aerial imagery, the Robertson lineation appeared to line up with a lineation making up the north edge of the Big Boiling Spring run (Figure 8). The Robertson lineation, measured using ArcGIS, is 236°. The lineation measured in the field at Big Boiling Spring is 220°. The length of apparent lineations on the Robertson property ranged from 69 – 2203 ft, with an average length of 353 ft.

Blackwell and Wells (1999) noted that resampling 1x1 m, bare-earth Lidar data to 5x5 m and 10x10 m cells allowed Lidar data to be more easily-processed. Resampling was not done on Bell County Lidar data because the karst features of interest would have been lost in a coarser-resolution dataset. The limitation of not resampling was that the volume of data was large, limiting the amount of data that could be processed at any given time and resulting in a smaller study area. While the 1x1 m resolution data confirmed the presence of the largest depressions and lineations on the Robertson property, the ability to identify smaller features, which may be important from a recharge perspective, is still limited.

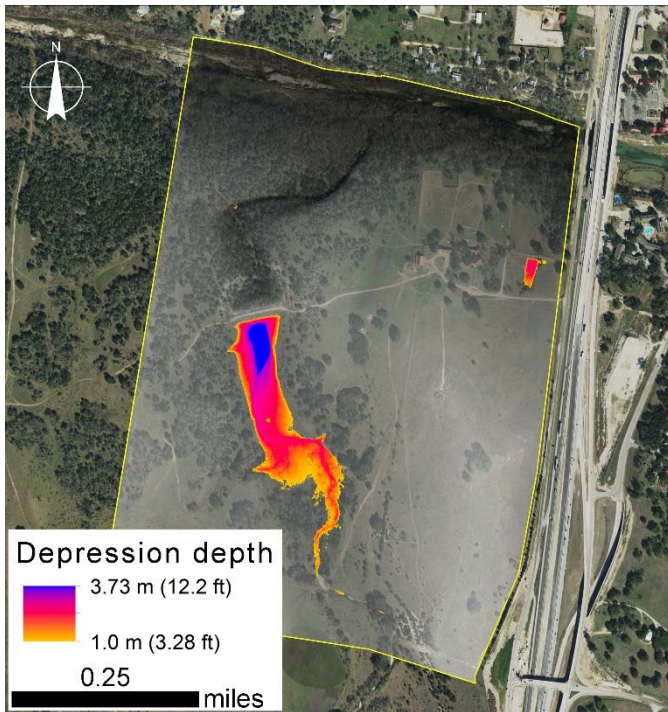


Figure 5. Map of depressions at Robertson Ranch, produced using semi-automatic sink determination.

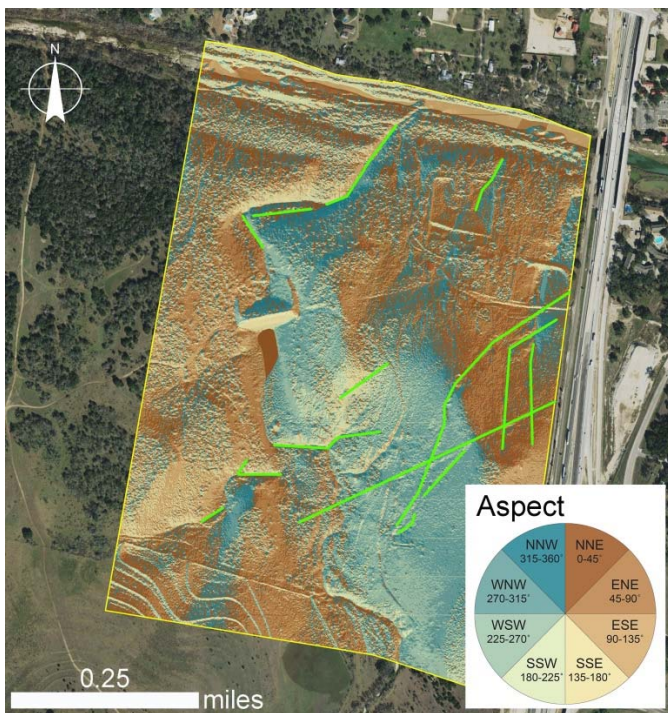


Figure 6. Aspect map of Robertson Ranch, with manually-determined lineations shown in green.

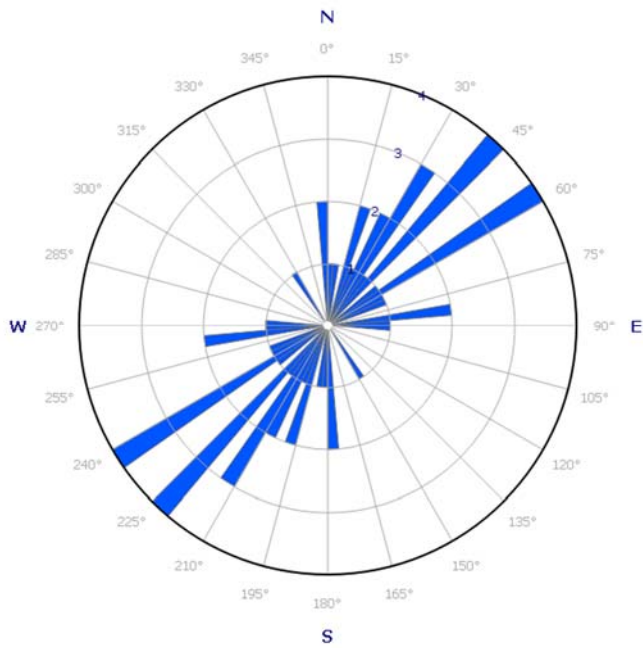


Figure 7. Rose diagram plotted using GeoRose 0.5.1 (Yong Technology Inc., 2015).

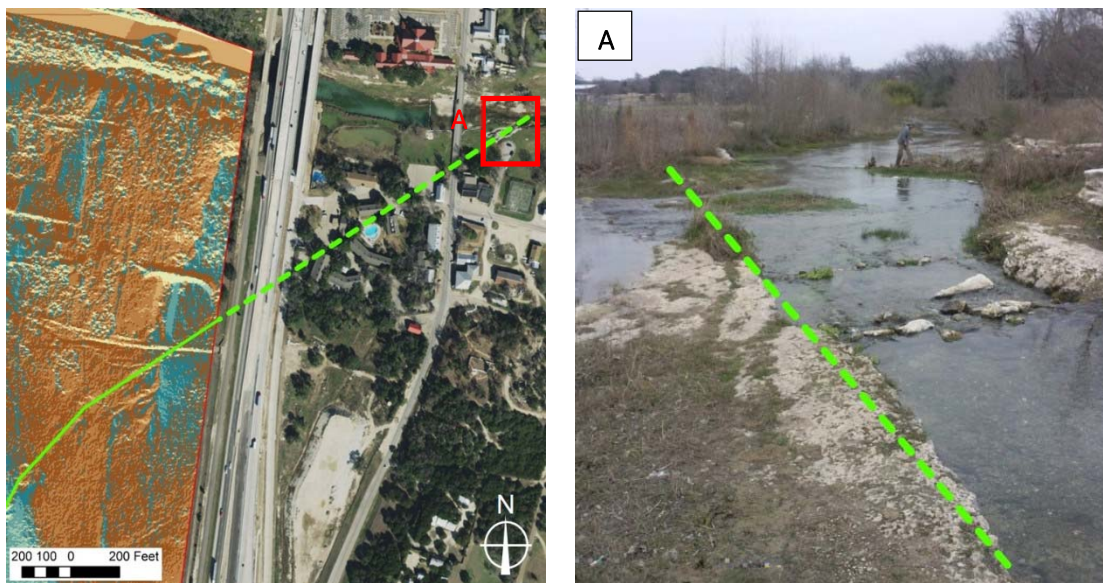


Figure 8. A major lineation extrapolated from Robertson Ranch, *left*, matches the field-determined orientation of a lineation observed at Big Boiling springs (A), *right*. Although the images were taken from different angles, the lineation from Robertson Ranch measured from ArcGIS is 236 degrees and the fracture lineation at Big Boiling Springs measured in the field with a Brunton Compass was 220 degrees. These orientations are closely aligned and fall in the range of the strongest trends on the Rose diagram.

Groundwater Monitoring

Multi-parameter monitoring

A data logger in a Northern Segment cave is being used to establish baseline levels of water level, temperature, and specific conductance; as well as to monitor response to precipitation events at this location in the Northern Segment. An OTT CTD datalogger (OTT Hydromet, Loveland, Colorado) was installed in the cave well underneath the Stagecoach Inn in Salado Texas on May 23, 2013. Measurements of water level (feet above the sensor), temperature ($^{\circ}\text{C}$), and specific conductance ($\mu\text{S}/\text{cm}$) were taken at an initial interval of logging a reading every 5 minutes, then adjusted to once every 10 minutes to conserve battery power and datalogger memory in May 2014. The datalogger was replaced with an identical OTT CTD datalogger with a longer vented cord on October 6, 2015.

A second multi-parameter sonde was installed on October 6, 2015 as a test for monitoring additional chemical parameters (Figure 9). An In-Situ Troll 9500 sonde and datalogger (In-Situ, Fort Collins, Colorado) was installed alongside the OTT CTD datalogger that has the ability to monitor pH, specific conductance ($\mu\text{S}/\text{cm}$), dissolved oxygen (mg/L or % saturation), and dissolved nitrate (ppm). Of particular interest is the change in groundwater nitrate over time. During a routine battery replacement on February 11, 2016, water seeped into the datalogger casing, causing the Troll 9500 to cease functioning. The entire unit was rebuilt and recalibrated over the following months, and re-deployed on September 1, 2016.

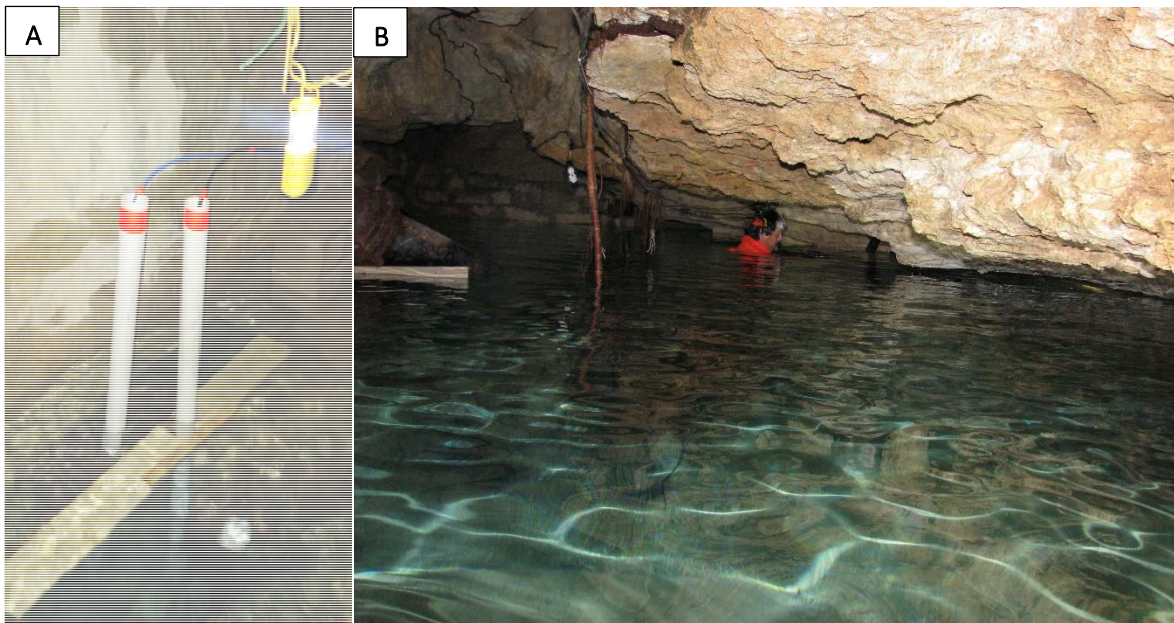


Figure 9. A multi-parameter datalogger has been deployed in the Stagecoach Inn cave well since May 2013 to collect data on water level, temperature, and specific conductance. (A) Setting of the OTT CTD (right side, black cord) and In-Situ Troll 9500 (left side, blue cord) sondes in the cave well. The sensors are set inside 2-inch PVC slotted near the bottom and attached to a wooden board for stability, with cinder blocks on top of the board to prevent movement during high water levels. The sondes are located in the lower portion of the PVC pipe which is screened. The dataloggers and connection ports are run along the cave wall to the foot of the stairs for easier access. (B) A large recharge event in May 2016 caused flooding in the cave; photo is of FWS biologist Pete Diaz retrieving a water sampler from the bottom of the cave well during high water levels.

Multi-parameter monitoring data

Long-term trends

Figure 10 shows daily water level, specific conductance, and temperature data from June 1st 2013 until September 21st 2016, giving an overview of hydrologic conditions in the Northern Segment at SCI cave over the past three years. Two notable gaps exist in the monitoring data collected by the OTT CTD datalogger. The first data gap occurs in May 2014 and was due to a loss of battery power. The datalogger was decommissioned on May 21st, brought back to Baylor University for routine maintenance and battery replacement, and re-deployed on June 1, 2014. The second data gap occurred in May 2015, when a large recharge event on May 26, 2015 dislodged the datalogger. It was therefore removed from the cave for the summer. An identical datalogger with a longer vented cable was re-deployed on October 6, 2015 to continue monitoring. Data collection has been consistent since then.

Water level ranged from 570.40 ft to 580.68 ft elevation, with an average of 573.81 ft elevation, or 19.44 ft below ground surface. Water levels increased after rains in late 2013 but returned to previous levels by late 2014. Since that time, rainfall and subsequent recharge have had a cumulative effect and the aquifer level has increased after rainfall events; following each rain, water level “stabilized” at a higher level compared to the previous water level. Over the recording period, overall water level increased; the first water elevation reading on June 2nd, 2013 was 571.64 ft and the last reading on September 21st, 2016 was 576.72 ft. Addition of water to the aquifer through recharge events are evident in peak responses in the hydrograph. The magnitude of response to recharge events appear to be greater in 2015-2016 than previously in the recording period, evident by sharper peaks in the hydrograph. Temperature values over the recording period remained fairly constant, ranging between 68.90°F and 69.93°F. The average temperature was 69.56°F. Sharp, temporary changes in temperature coincided with recharge events and the introduction of rain water that reflect the ambient surface air temperature (that is, colder rain water during winter months and warmer rain water during summer months). Specific conductance values, which are related to the concentration of ions dissolved in water, ranged between 544 $\mu\text{S}/\text{cm}$ and 606 $\mu\text{S}/\text{cm}$ over the recording period, with an average value of 580 $\mu\text{S}/\text{cm}$. Sharp drops in specific conductance were observed shortly after each rain event, and then increased as water levels receded. The drops may reflect introduction of lower-specific conductance rainwater, producing a dilution effect. Inversely, as water level declines over a dry season, specific conductance increases.

High-resolution data

Examining high-resolution monitoring data collected at 15-minute intervals allows a closer look at recharge response of the Northern Segment at SCI cave. An example of such data is provided for May 2015 (Figure 11). Aquifer response to recharge appears to be a function of both the amount of rainfall, antecedent moisture and possibly the location within the basin. By coupling data logged in the SCI cave well with precipitation data, smaller rains were observed to have little or no effect on temperature and specific conductance (Figure 11; contrast locations *A* and *B* with location *C*), while all rainfall caused change in water level to some degree. Antecedent moisture refers to the relative wetness of the unsaturated zone preceding a rain event. If a given rainfall is preceded by a long dry period, the antecedent moisture of the unsaturated zone will be low and any rainfall will fill pores in the zone instead of infiltrating by gravity to the water table. However, if the time is short between rain events, antecedent moisture will be high (that is, the zone will be near saturation). More rain will infiltrate to the water table, and an increase in aquifer level will be observed. The impact of antecedent moisture conditions on groundwater recharge has been documented in other studies such as those of Zhang and Schilling (2006), and Sorman and Abulrazzak (1993); it was also observed at SCI cave. The effect of antecedent moisture on groundwater level may be observed by contrasting a 0.3” rain event on May 12th (Figure 11; location *A*) and 0.17” rain event on May 14th (Figure 11; location *B*). Water level rose less than two inches at SCI cave after the May 12th rainfall; meanwhile, despite less recorded rainfall on May 14th, water level rose about four inches. A slight lag time between change in water level preceding any change in temperature or specific conductance (Figure 11; location *C*) suggests that recharge entered the aquifer at some point away from the SCI cave, changing head in the aquifer and displacing

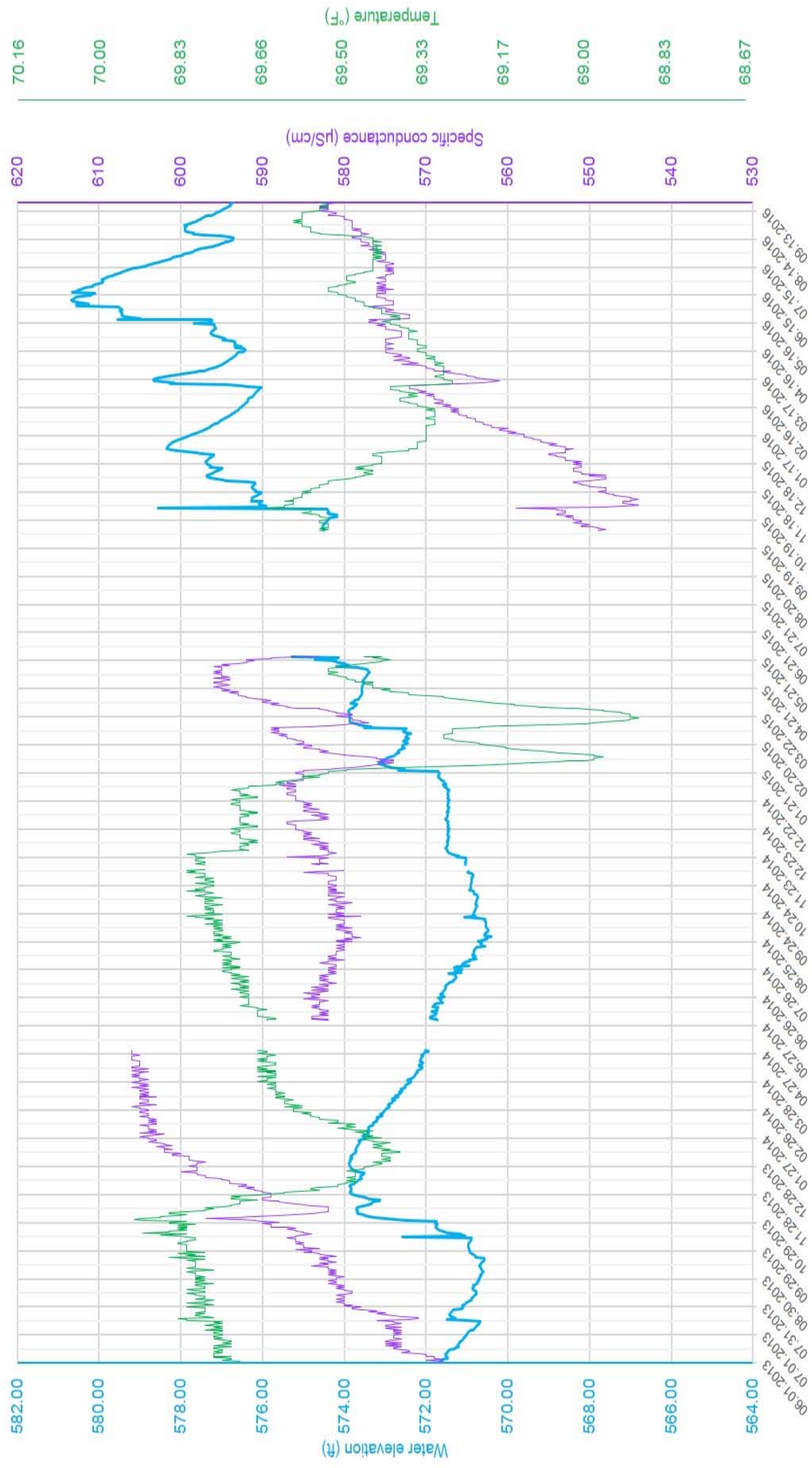


Figure 10. Hydrologic conditions at the Stagecoach Inn cave well from June 2013 to September 2016. Daily values are plotted.

antecedent water. Water level at SCI cave responds to the addition of water, while temperature and specific conductance remain unchanged until new water flows through the cave.

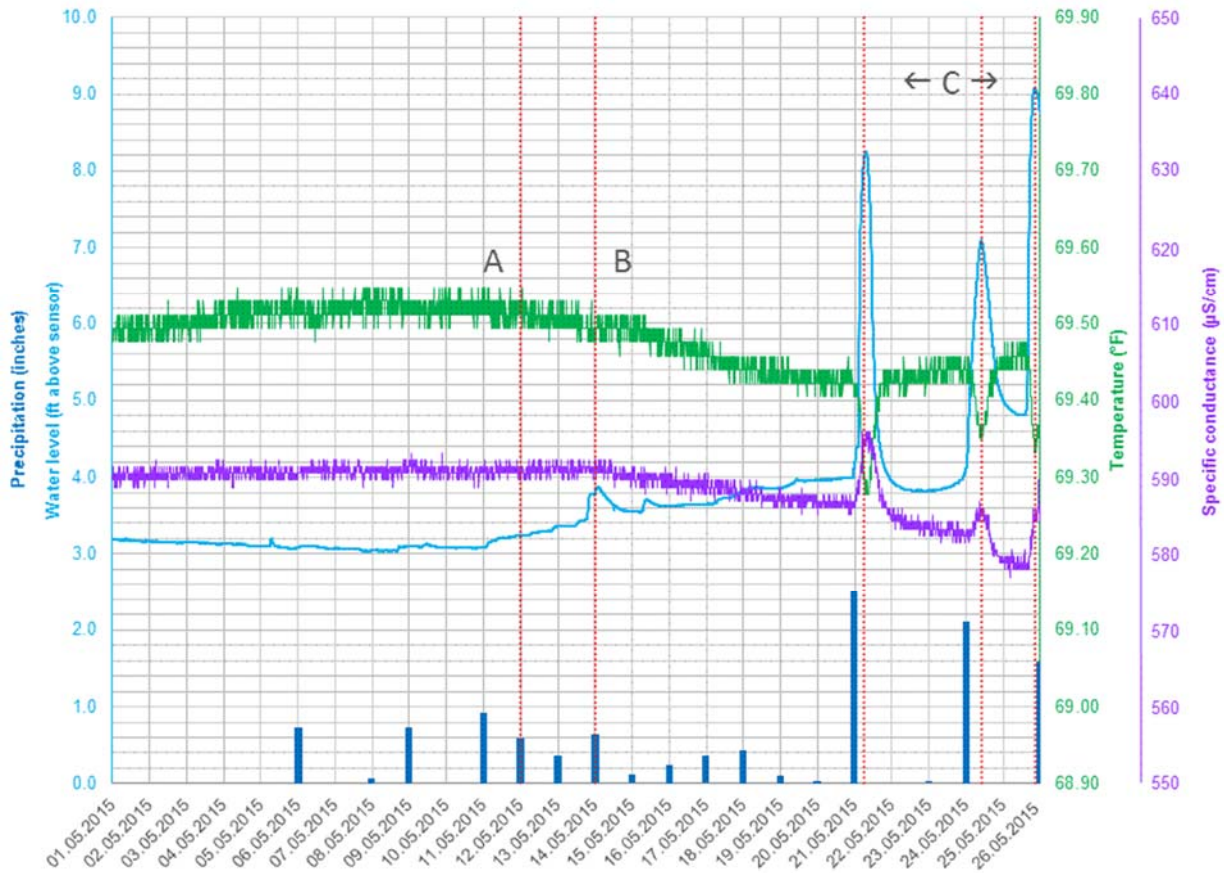


Figure 11. Hydrologic conditions at the Stagecoach Inn cave well in May 2015. Water level, temperature, and specific conductance measurements were logged every 15 minutes. Rainfall data from the nearest NOAA WSR-88D station (Geo ID #609938) are plotted as bars.

Nitrate monitoring

Monitoring data (Figures 12) show that nitrate levels in the aquifer appear to respond to episodic loading or recharge events, and return to pre-episode levels within a few days. From the monitoring conducted in this study, nitrate levels do not appear to exhibit an increasing trend through time; however, the monitoring period was short (a few months), and a longer monitoring period may provide a better perspective.

Initial monitoring data collected from October to November of 2015 (Figure 12) prompted additional grab sampling before, during, and after high-traffic weekends (ie, holiday or Salado event weekends). Conceptually, nitrate concentrations in groundwater should be low before a high-traffic weekend, highest during the weekend, and returning to a low level after the weekend; this was observed in the initial data (Figure 12; see locations A, B, and C). The objective of grab sampling was: 1) to obtain more accurate nitrate concentrations, as the Troll 9500 functions better as a trending instrument; and 2) to see if nitrate concentrations would correlate with the increase and decrease of nitrate as recorded by the Troll 9500.

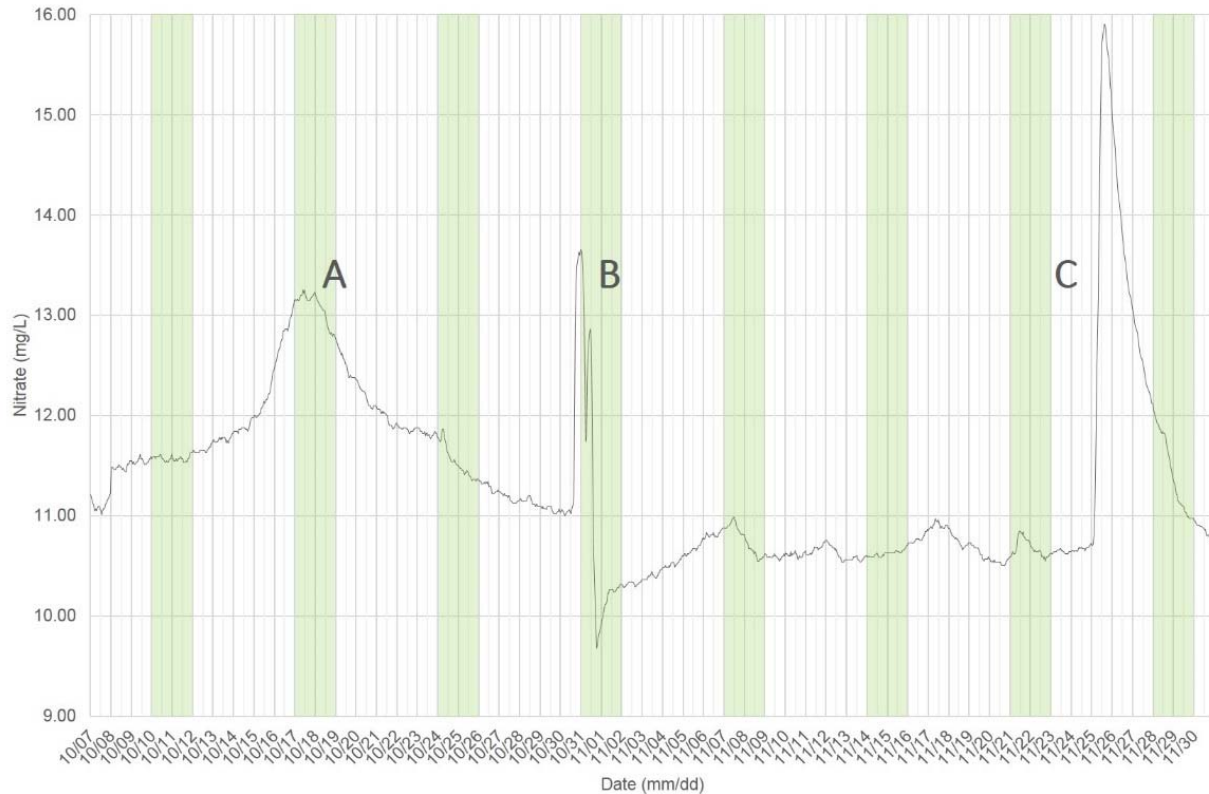


Figure 12. Nitrate trend data collected by the Troll 9500 sonde from October 7 to November 30, 2015 at the Stagecoach Inn Cave well. Green-shaded days indicate weekends (Saturday-Sunday). The spikes at A, B, and C correlate with high-traffic weekends in Salado; A correlates with the Halloween Fright Trail, B correlates with Halloween, and C correlates with Thanksgiving.

Methods

Grab-sampling was conducted over the following weekends: Easter (March 23-30), Labor Day (September 1-8) and the Salado Chocolate and Wine Weekend (September 14-21). Grab-sampling was also conducted over a low-traffic weekend on February 11-16 (ie, not a holiday or Salado event weekend) as a control. Samples were collected before the weekend on either Wednesday or Thursday, during the weekend on Saturday, and after the weekend on Wednesday or Thursday. During each sampling event, water was collected from each downtown spring outlet (Big Boiling, Little Bubbly, Side, Critchfield, Doc Benedict, and Anderson Springs), Salado Creek upstream of the spring complex at Main Street Bridge and downstream of the complex at Inn on the Creek, and Stagecoach Inn Cave. Forty milliliters of water were filtered through a 0.45 μm syringe filter, and collected in triple-rinsed 50 ml PPE centrifuge tubes. As quality controls, a trip blank and field blank were collected on each sample day, and one site was randomly selected to collect a duplicate sample. Samples were stored in ice and transported back to the Baylor CRASR (Center for Reservoir and Aquatic Systems Research) lab for analysis.

Results and Discussion

Results from all sampling events are tabulated in Appendix A. A summary of sampling locations and mean nitrate concentrations are provided in Figure 13. Surface water just upstream from the downtown springs has an average nitrate concentration of 1.93 mg/L. The springs are a source of nitrate input to Salado Creek; all sampled springs had average nitrate concentrations between 3.10-3.50 mg/L. Surface water downstream of the springs contains an average 2.28 mg/L nitrate, reflecting the addition of nitrate from groundwater.

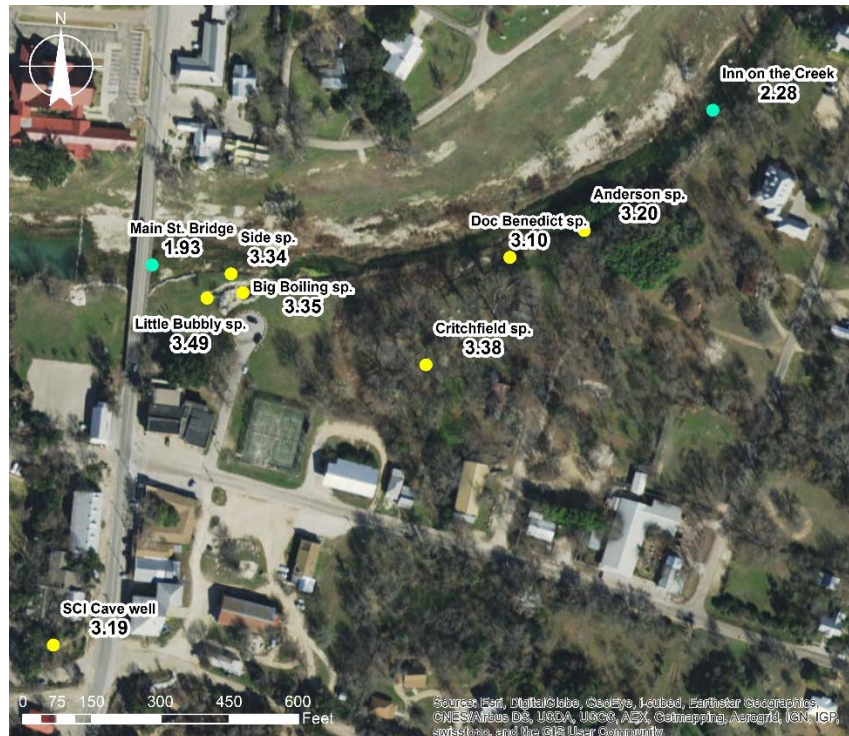


Figure 13. Map of nitrate sampling locations around downtown Salado showing average nitrate concentrations from all sampling events in mg/L. Specific nitrate concentrations for each event can be found in Appendix A.

Nitrate concentrations from the Labor Day long weekend sampling are shown in Figure 14. It is evident that quite a few of the sampling locations exhibit the low-high-low pattern, again supporting the observation that nitrate content in the Salado Springs complex be influenced by high-use, episodic loading. Measured nitrate concentrations for all surface water and groundwater sample locations ranged from 1.19 mg/L to 3.84 mg/L, with a mean concentration of 2.71 mg/L. At groundwater sampling locations (ie, the springs and the Cave well), nitrate concentrations ranged from 1.88 mg/L to 3.84 mg/L, with a mean concentration of 2.99 mg/L.

Critchfield spring is notably different from other springs, exhibiting a high-low-high pattern. We know from eye-witness accounts (Tim Brown, personal communication) that Critchfield Spring developed as a result of excavation in the area for Mr. Critchfield’s fish pond as opposed to natural exposure. As a result, Critchfield Spring, while being hydrologically connected to other springs in the downtown Salado Complex (established through dye tracing), is slightly different in geomorphologic setting and chemistry. Taking Critchfield Spring out of the statistical analysis for nitrate concentration does not change the range observed in groundwater sampling points; however, the mean concentration is 2.97 mg/L which is slightly lower.

Measured nitrate concentrations in the Salado Springs complex is within the range of nitrate measured in the unconfined portions in the San Antonio and Barton Spring segments of the Edwards BFZ aquifer. Krietler and Browning (1983) measured groundwater nitrate concentration as well as nitrogen isotopes in both the unconfined and confined portions of the San Antonio Segment. Nitrate concentration in unconfined groundwater ranged from 1.8-190 mg/L, but only two samples had concentrations greater than 15 mg/L (190 mg/L in a Bexar County well, and 29.0 mg/L in a Medina County well). Without these two high values, groundwater in the unconfined portion of the San Antonio Segment ranged from 1.8-14.9 mg/L, with a mean concentration of 7.06 mg/L and a median concentration of 6.1 mg/L. Slade and others (1986) assessed the hydrology and water quality of the Edwards Aquifer at Barton Springs. They reported a nitrate concentration of 1.0 mg/L for three samples collected between 1941 and 1955. Samples collected for the 1986 assessment contained a mean nitrate concentration of 1.5 mg/L. Slade and

others suggested that the increase in nitrate could be due to cattle and septic tanks, sanitary sewer systems in residential developments, or privately-owned sewage-treatment plants. Slade and others also observed highest nitrate levels in shallower wells, or wells located in the recharge area of the aquifer.

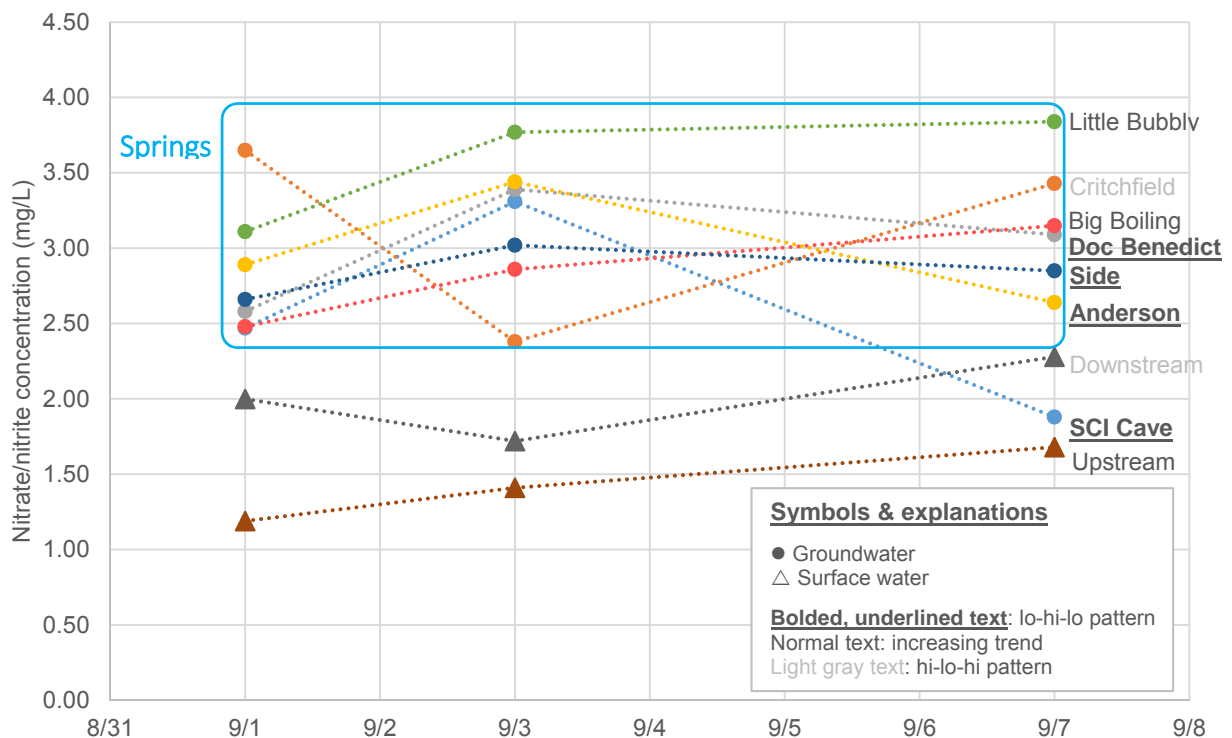


Figure 14. Nitrate concentrations at Salado Springs over the Labor Day long weekend (September 1st, 3rd, and 8th). Each spring outlet was sampled, as well as points upstream and downstream of the downtown spring complex.

Surface water appears to have a lower concentration of nitrate than groundwater. Because Salado Creek is a baseflow, perennial stream that is fed primarily from springs and seeps sourced from the Edwards aquifer, the lower concentration may be the result of plants taking nitrogen out of solution as a grown nutrient. Much of the nitrogen may return to the water when the plants senesce in the winter.

Grab-sample concentrations were compared to the Troll 9500 monitoring data, and did not seem to correlate well in the amount of nitrate detected nor in temporal trend. While nitrate concentrations do appear to increase during weekend events, they do not appear to correlate to the timing of nitrate peaks recorded by the Troll 9500 (Figure 15). It was not expected for the magnitude of nitrate to be comparable; nitrate sensors in general have difficulty remaining calibrated. However, the hope was that the nitrate sensor could provide trend data and indicate times to collect grab-samples, which could then be analyzed using lab techniques to obtain accurate nitrate concentrations.

The nitrate sensor on the Troll 9500 did not give accurate or dependable trend results.

- a. The sensor measured concentrations larger than the chemical analysis of the same water
- b. Grab sampling during sensor peaks was not consistent and did not show the same trends as the Troll 9500.

The nitrate sensor is difficult to calibrate and maintain. Therefore, it is probably more effective to collect periodic water samples to be analyzed in a lab and monitor for temporal changes.

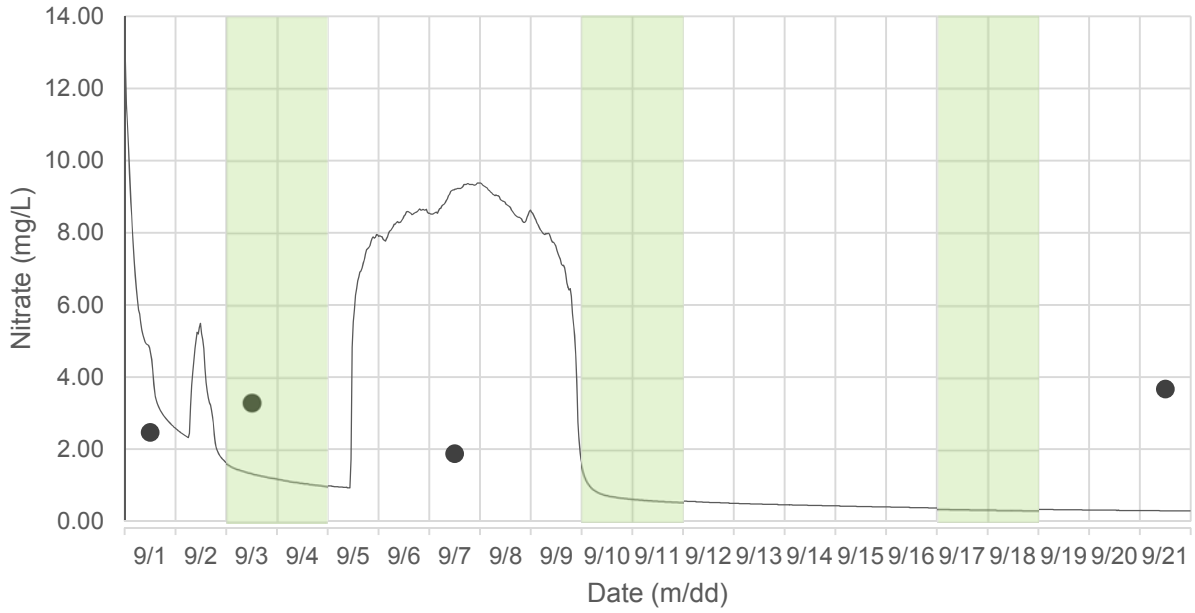


Figure 15. Nitrate trend data collected by the Troll 9500 sonde and grab samples from September 1-21, 2016 at the Stagecoach Inn Cave well. Points represent nitrate concentrations for grab samples collected from Stagecoach Inn Cave over the labor day long weekend and after the Salado Chocolate and Wine Weekend event. Green-shaded days indicate weekends (Saturday-Sunday).

Groundwater-surface water interaction

Stream Profiling

Profiling Salado Creek at three cross-sections near Big Boiling Spring has continued. Cross-sectional profiling helps to monitor physical and chemical conditions, as well as comparison with previously-collected data (water depth, temperature, and specific conductance) at Salado Creek. Flow measurements were also taken.

The three cross-sections were located in Salado Creek (Figure 16): within the spring flow of Big Boiling Spring (cross-section one), in Salado Creek upstream of the confluence of Big Boiling Spring (cross-section two), and in Salado Creek downstream of the confluence of Big Boiling Spring (cross-section three).

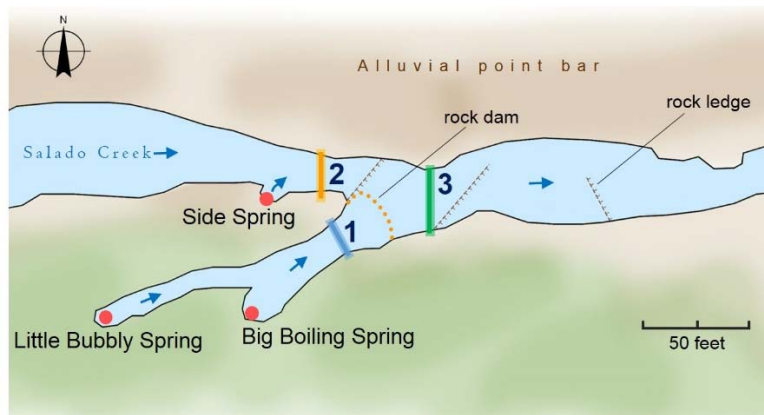


Figure 16. Diagram of downtown Salado Creek showing key features. The area around Big Boiling Spring, Little Bubbly Spring, Side Spring, and the adjacent section of Salado Creek was the focus of the study. Cross-section locations used for stream profiling are indicated by the colored lines and labelled 1, 2, and 3.

Methods

All three cross-sections were taken perpendicular to flow direction. The measured parameters included: depth in feet (ft.), temperature in degrees Celsius (°C), specific conductance in micro-Siemens ($\mu\text{S}/\text{cm}$), and flow in feet per second (fps). Measurements were made across the creek using stadia rod or reel tape laid across the channel width. Depth was measured using a metal yard stick. Temperature and specific conductance were measured using a Solinst TLC meter (Solinst Model 107 TLC Meter; Solinst Canada Ltd., Georgetown, Ontario). Flow was measured using a SonTek Flowtracker (SonTek, San Diego, California). The discharge at each profile was calculated using the midsection method, a standard discharge calculation method utilized by SonTek/YSI Inc. and the U.S. Geological Survey (SonTek, 2007). The midsection method assumes that a measured velocity is representative of the mean velocity for a rectangular segment of a stream profile (Turnipseed and Sauer, 2010). The partial discharge at each rectangular segment is calculated using the following formula, then summed to determine the total discharge of the stream profile (Turnipseed and Sauer, 2010).

$$q_i = v_i \left[\frac{b_{(i+1)} - b_{(i-1)}}{2} \right] d_i$$

where q_i is the partial discharge through section i , v_i is the mean velocity at location i , $b_{(i+1)}$ is the distance from the starting point of the profile to the next location, $b_{(i-1)}$ is the distance from the starting point to the preceding location, and d_i is the depth of water at location i .

The specific conductance measurements were made in the natural water environment without the use of a stilling well or container, and without filtering the water. The water was very clear (spring flow and base flow conditions) but was flowing briskly except near the stream banks.

Results and Discussion

Cross-section one is characterized by unusual spatial consistency in temperature and specific conductance (Figure 17). Flow velocity ranged from 0.0381 ft/s towards the left edge-of-water of the Big Boiling spring run, to 0.351 ft/s towards the center of the profile. The average velocity was 0.2343 ft/s, and total discharge at cross-section one was calculated to be 5.0 cfs. Specific conductance and temperature readings were consistent across the profile. Specific conductance measured 483 $\mu\text{S}/\text{cm}$ across the profile except from 3-6 ft where specific conductance was 482 $\mu\text{S}/\text{cm}$, and temperature measured 20.9°C across the profile. Steady depth and temperature values are understandable for a spring flow discharge channel and the landscaped, un-shaded nature of the Big Boiling spring run. The slight changes in specific conductance may be the result of variability in flow velocities that could affect the reading. Similar specific conductance values suggest a single source of water; in this setting it is groundwater discharging from Big Boiling Spring. Furthermore, specific conductance values are similar to those measured at the Stagecoach Inn Cave, located to the south and up-gradient with regard to groundwater flow. The similar specific conductance values suggest that Big Boiling Spring and the Stagecoach Inn Cave are part of the same groundwater system.

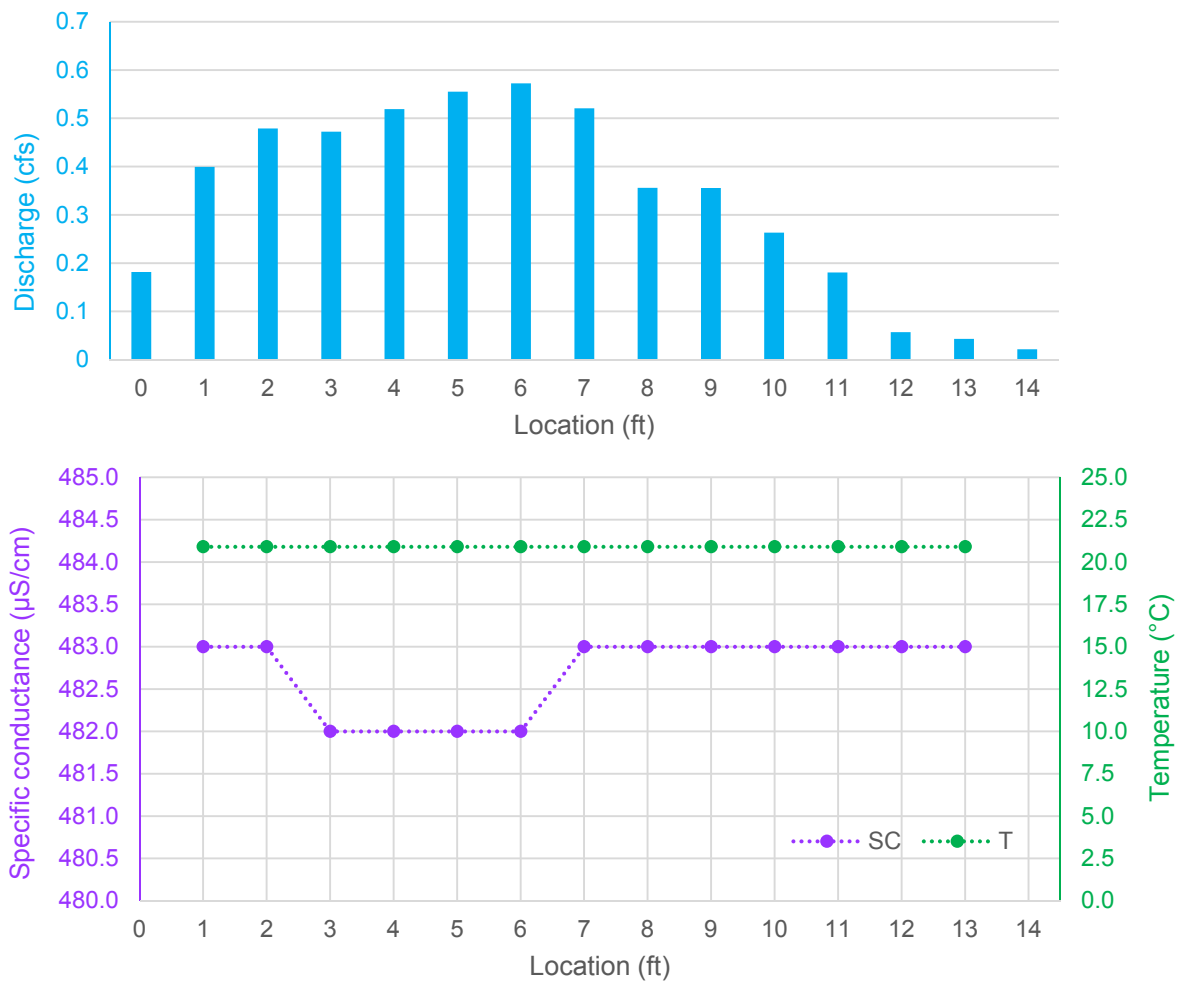


Figure 17. Discharge (*top*), specific conductance and temperature (*bottom*) measurements at cross-section 1, located in the spring flow of Big Boiling Spring. Measurements were taken on July 29, 2016.

Cross-section two is located in the natural channel of Salado Creek, upstream from Big Boiling Spring (Figure 18). Flow velocity ranged from 0 ft/s at the north bank of Salado Creek (left edge-of-water; 28 ft) which is a gently-sloping alluvial point bar, to 2.1962 ft/s near the south bank of Salado Creek (4 ft), where the thalweg is located. The average velocity was 1.1338 ft/s, and total discharge at cross-section two was calculated to be 28.7 cfs. Specific conductance ranged from 430 to 442 $\mu\text{S}/\text{cm}$; the average value was 433 $\mu\text{S}/\text{cm}$. Temperature ranged from 23-24.7°C; the average value was 23.7°C. The cross-section is consistently shallow, with comparatively warm water and lower specific conductance relative to cross-section one. Temperature and specific conductance values were again fairly consistent across the section. Increased in temperature and decreased specific conductance near the north bank (feet 27-30) are the result of very shallow, muddy conditions. In contrast, decreased temperature and increased specific conductance near the south bank (feet 1-2) suggest groundwater influence, possibly through bank seepage. Overall, higher temperature and lower specific conductance values than those measured at cross-section 1 suggest that flow in Salado Creek upstream of Big Boiling Spring is dominated by streamflow rather than direct groundwater. Although flow in Salado Creek during these observations was dominated by baseflow from groundwater, a low-water dam immediately upstream is partly responsible for increased temperatures and lower specific conductance.

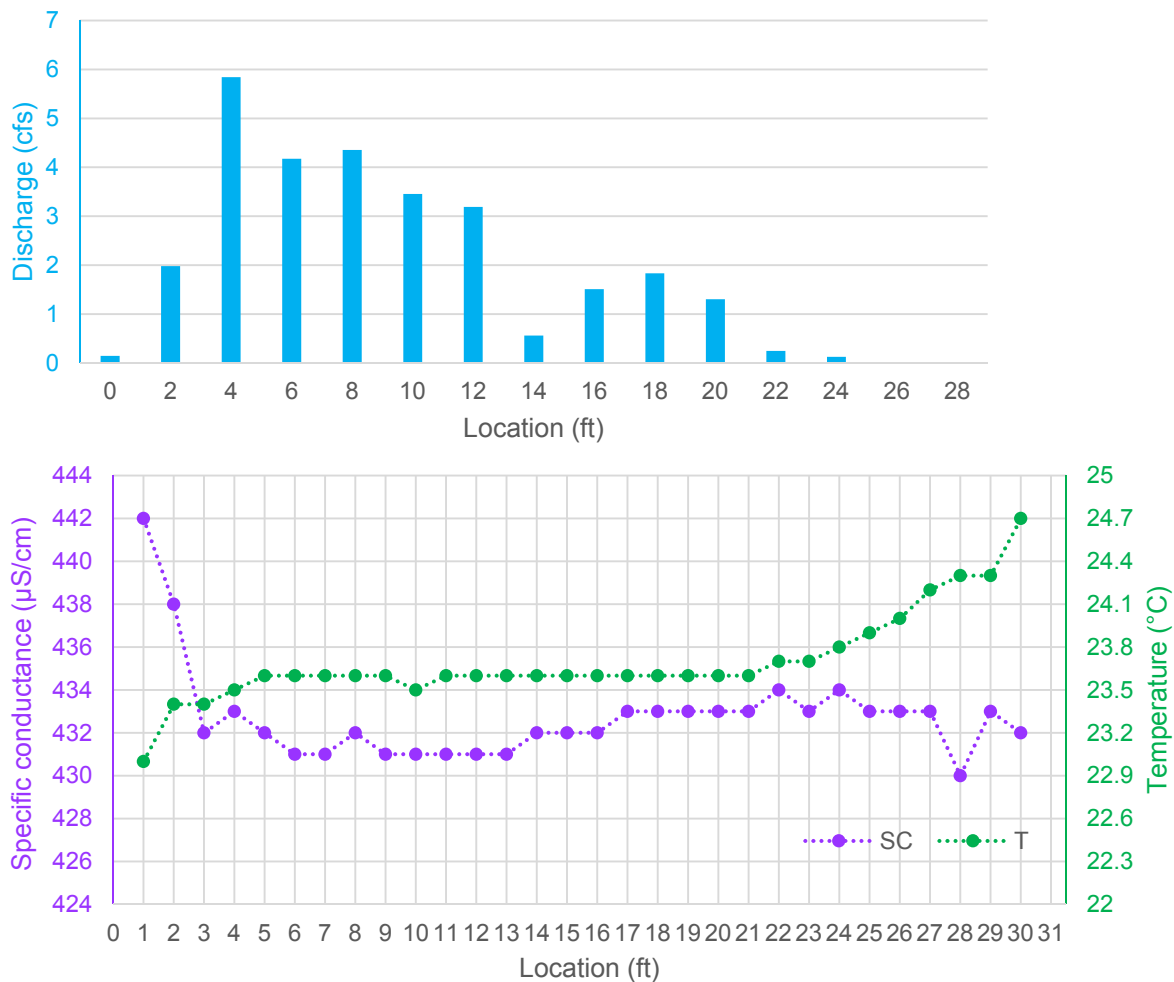


Figure 18. Discharge (*top*), specific conductance and temperature (*bottom*) measurements at cross-section 2, located in the natural channel of Salado Creek. Measurements were taken on July 29, 2016.

Cross-section three is located in the natural channel of Salado Creek, downstream of the confluence with Big Boiling Spring (Figure 19). Flow velocity ranged from 0 ft/s at the north bank of Salado Creek (left edge-of-water; 44 ft)

which is an alluvial point bar, to 2.6362 ft/s (26 ft). The average velocity was 1.5569 ft/s, and total discharge at cross-section two was calculated to be 34.0 cfs. The flow distribution at cross-section three is bimodal, reflecting the contribution of groundwater to Salado Creek at this location. The peak centered at 4 ft is primarily groundwater flow from Big Boiling Spring, while the peak centered around 28 ft is surface water from upstream. Specific conductance ranged from 420 to 483 $\mu\text{S}/\text{cm}$; the average value was 442 $\mu\text{S}/\text{cm}$. Temperature ranged from 21.2-23.7°C; the average value was 23.0°C. Temperature and specific conductance values at this location exhibit a larger range than cross-sections one or two. This is to be expected since cross-section three is influenced by both spring and stream flow. Temperature and specific conductance at this location are intermediate values of those measured at cross-sections one and two, suggesting a mixing of stream water (represented by cross-section two) and groundwater discharging from Big Boiling Spring on the south side of the channel (represented by cross-section one). The width of groundwater influence is clearly evident in temperature and specific conductance values from 1 ft to about 8 ft of the cross-section, which are similar to measurements from Big Boiling Spring. The temperature rises and specific conductance decreases from the south to the north in the middle section as more surface water influences the total water flow. Since the burial of Rock Spring at north bank in the spring 2016, groundwater influence on temperature and specific conductance values is no longer evident.

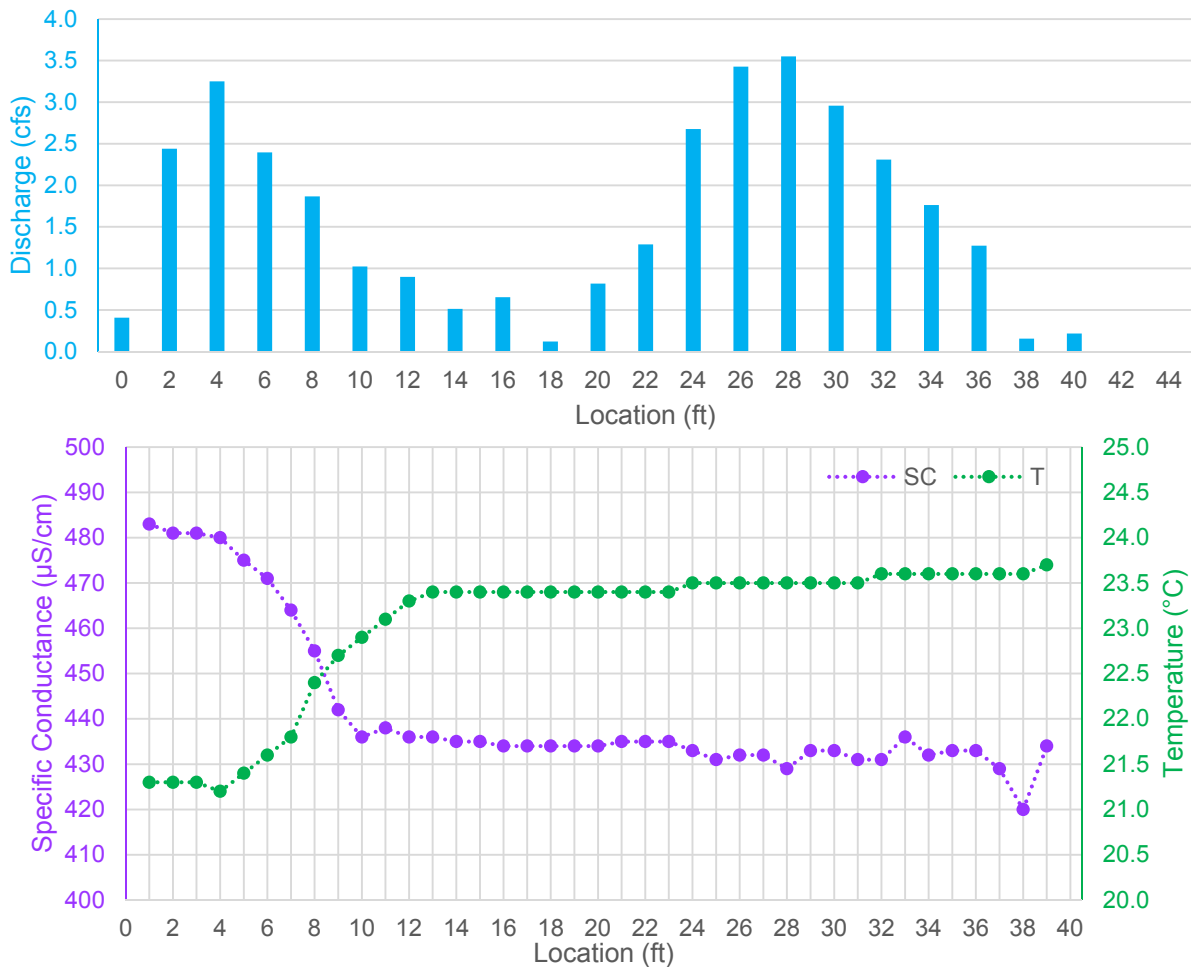


Figure 19. Discharge (*top*), specific conductance and temperature (*bottom*) measurements at cross-section 3, located in the natural channel of Salado Creek, downstream of the confluence with Big Boiling Spring. Measurements were taken on July 29, 2016.

Thermography (FLIR)

Habitat for the Salado Salamander is associated with springs in the Northern Segment of the Balcones Fault Zone Edwards aquifer. However, questions remain as to how far back into the aquifer and how far beyond the spring orifices suitable habitat may occur. Temperature is quite consistent within the aquifer and has always been a critical habitat factor but determining the temperature consistency beyond the spring orifice can be difficult and time consuming. Differences between surface water and groundwater can be visible immediately after rains when sediment from runoff is suspended in the surface water but groundwater discharging from the springs remains clear (Figure 20). However, after the runoff event ends, the sediment settles out and the stream flow is supported primarily by baseflow which appears clear and is difficult to distinguish visually from the groundwater discharge (Figure 21). An infrared camera capable of measuring and displaying temperatures over an area was useful for providing insight into the extent of groundwater-dominated temperatures in spring runs, receiving streams, and the types of groundwater/surface-water interactions that may occur. Additionally, stream portions influenced by groundwater temperatures were observed to contain vegetation associated with springs and potential salamander habitat.

Because no published literature existed on the temperature distribution within this specific area of Salado Springs, the first efforts consisted of data gathered with a handheld FLIR-E63900 Infrared camera (Figure 22; FLIR® Systems, Inc.). The camera setting for emissivity did not change during the study but stayed as a constant setting of 0.95 which is thought to represent the emissivity of water. Distance settings were estimated for each image and ranged from 3-16 meters. When air temperatures were less than 40°F, the cold air absorbed some of the infrared energy over distances greater than about 10 meters and resulted in poor results. The spot check feature was used and the spot values compared closely with temperatures of the water measured with a probe. On January 22, 2016, the spot check on the FLIR was compared against temperatures measured using the Solinst TLC meter, which was also used for stream profiling. The temperature at the Big Boiling Spring orifice measured with the Solinst meter was 20.7°C while the FLIR spot check registered 20.9°C. Little Bubbly Spring measurements that day were 20.6°C at the orifice with the Solinst and 20.6°C with the FLIR. Because the water of greatest interest was groundwater discharging from a given spring, the spot check feature was used as both a hot spot and as a cool spot depending upon the type of temperature contrast between the groundwater from the springs and the surface water in the stream.

When the water is clear, temperature measurements and the FLIR camera can be used to determine the extent of groundwater/surface-water interactions. Essentially, in the summer when the air temperatures are high and the sun warms the surface water, groundwater is significantly cooler than the surface water; and in the winter when the air temperatures are cold and the surface water is also cold, then groundwater is relatively warmer. An example FLIR camera image compared to the visible light digital camera image can be seen in figure 23. In this figure, Side spring is discharging into Salado Creek when the groundwater from Side Spring is warm (68.5°F) and the surface water of Salado Creek is much cooler (47.2°F).

In addition to infrared imaging, profiles of temperature (T) and specific conductance (SC) along cross-sections in the Big Boiling spring run, and in Salado Creek upstream and downstream of the confluence of Big Boiling Spring were compared to the FLIR images to better understand temperature trends in relation to water flow and perhaps the chemistry as well. The study area focused on the area upstream and downstream of Big Boiling Spring although it included Side Spring and Little Bubbly Spring as well. Figure 16 shows the focus area. Temperature and specific conductance profiles were measured on April 6, 2016, in the area around Big Boiling Springs for direct comparison to FLIR images.



Figure 20. Abrupt contrast between clear groundwater flowing from Big Boiling Springs and sediment-laden surface water in Salado Creek after a small rainfall and during low spring flow conditions (October 7, 2013).



Figure 21. No contrast between clear groundwater flowing from Big Boiling Springs into clear baseflow in Salado Creek (July 31, 2013).



Figure 22. FLIR E63900 handheld infrared camera.

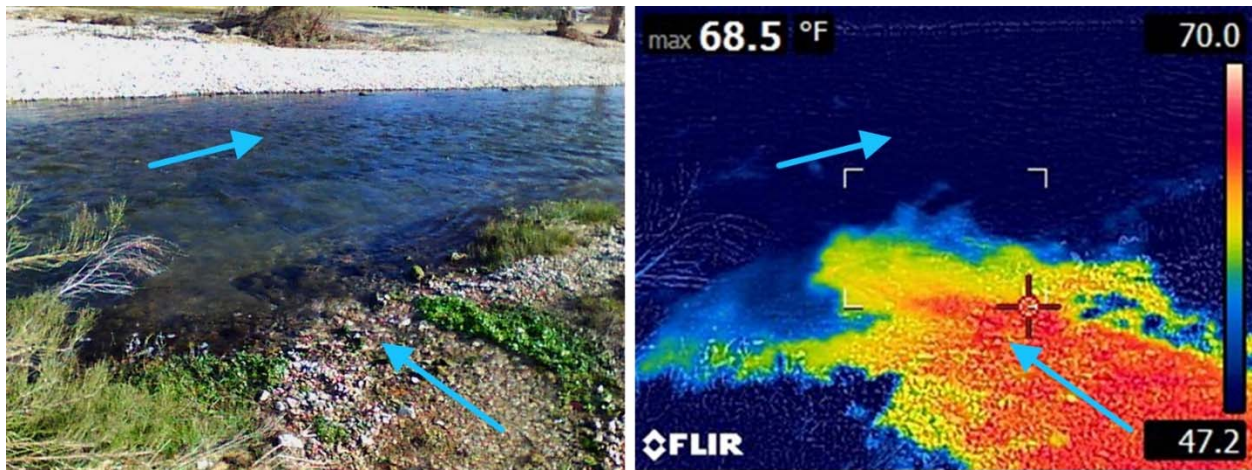


Figure 23. Side Spring looking northward from the south bank of Salado Creek in downtown Salado, Texas (January 27, 2016). The *left image* is a digital photograph and the *right image* is the infrared photograph showing temperature distribution. In the visible light image (*left*) it is impossible to see the boundaries and extent of the groundwater from Side Spring but these are readily observed in the infrared image below.

The temperature profile values showed remarkable consistency in Section 1 (Big Boiling Spring run). Section 2 which is upstream of Big Boiling Spring discharge also shows a consistent but cooler temperature profile than Section 1 with the exception of shallow water warming effects near the left edge-of-water (LEW), or north bank. Section 3 contains more overall variability than sections 1 and 2 but shows a shallow water warming trend on the LEW edge similar to Section 2. However, there is a warm water section about 4 feet wide along the right edge-of-water (REW) in Section 3 that did not appear on Section 2, and the magnitude of those temperatures match the temperatures for Big Boiling Spring discharge (Figure 24).

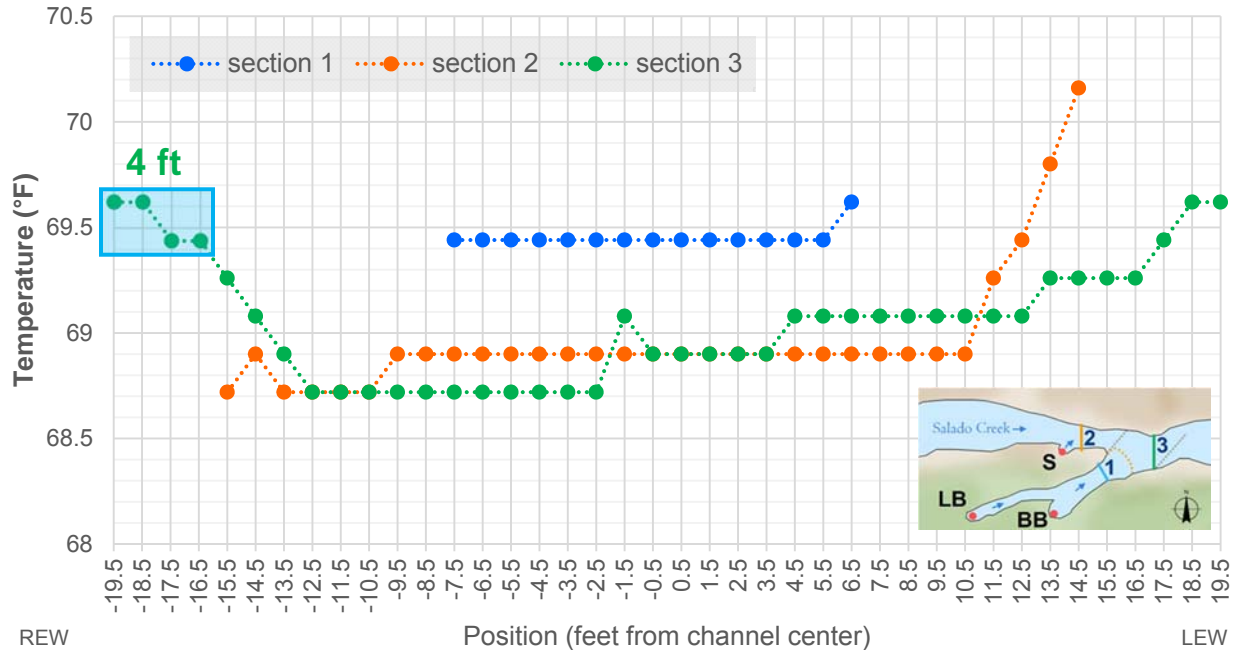


Figure 24. Temperature profiles in Salado creek and Big Boiling Spring, April 6, 2016.

The specific conductance profile measured on April 6, 2016 showed the same 4-foot wide area on the REW stream bank that the T profile showed, but in an even more dramatic fashion (Figure 25). The FLIR image also showed a 4-foot wide area of warmer temperatures on the REW side of the stream (Figure 26). The temperature values from the FLIR image are a few degrees lower than those recorded with the probe. The groundwater has not mixed with the surface water at this point downstream from the spring discharge. In addition, *Ludwigia*, a plant indicative of spring flow and known to provide habitat for salamanders, was found in this 4-foot section of the stream dominated by spring discharge (Figure 27).

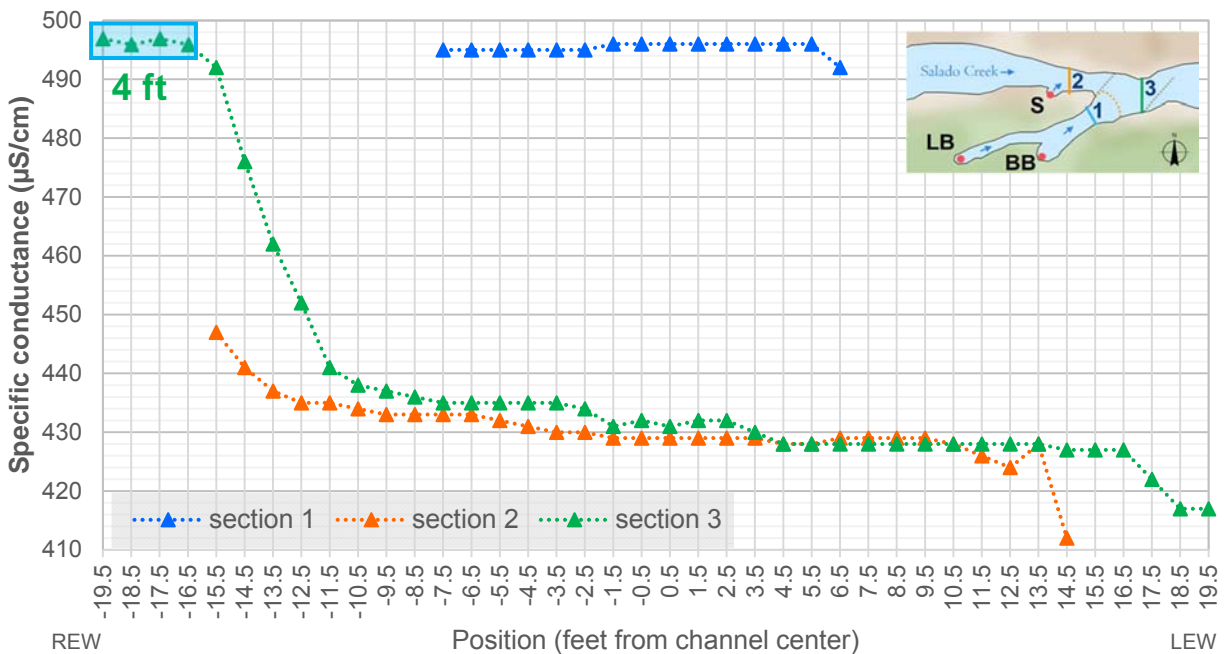


Figure 25. Specific conductance profile at section 3 April 6, 2016.

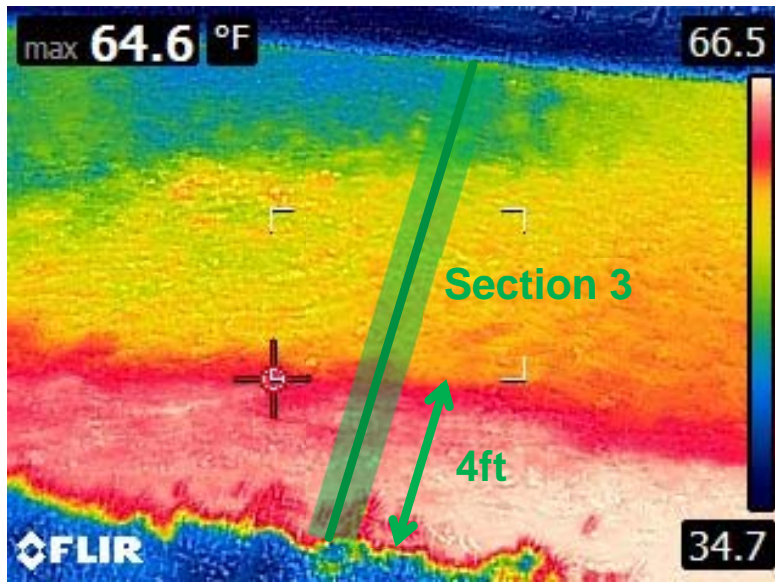


Figure 26. FLIR infrared image of profile Section 3 downstream from Big Boiling Spring showing the warmer temperatures associated with the groundwater discharge of Big Boiling Spring along the REW edge of the creek.



Figure 27. *Ludwigia* (submerged reddish plant) growing near the REW bank of Salado Creek downstream from the spring discharge of Big Boiling Spring, April 6, 2016.

Discussions and conclusions regarding the FLIR camera

The camera produces dramatic images that can be used to better understand interactions between groundwater and surface water. Although the spot check feature can produce similar temperatures to measurements from thermistors or thermometers, the FLIR readings represent surface temperatures and are most appropriate for shallow water where temperatures do not change drastically between the top and bottom of the water column. The infrared imagery is most efficient when there are drastic differences in temperatures between subjects of interest. When studying springs and interactions between groundwater and surface water in Central Texas, winter and summer are the preferred seasons compared to spring and fall. If the technology is used for locating groundwater

discharge during summer, it is best to do the field work in the morning and if working in the winter it is best to use the camera late in the day. Before dawn and after dusk are tempting application times, but the low lighting loses the ability to use visible light images for direct comparison.

The study showed variability in the stream areas impacted by groundwater discharge over time. The area affected by groundwater temperatures and chemistry (SC) was dependent upon the amount of spring discharge in relation to the amount of stream discharge. Big Boiling Spring has a larger impact area than Side Spring because its discharge is greater. Salado Creek is a fairly “flashy” stream, and during floods, the stream is the dominant flow contributor and groundwater does not impact a large area. However, groundwater levels rise quickly in conjunction with stream levels during floods and surface water does not appear to affect the T or SC of groundwater. The presence of *Ludwigia* and other vegetation indicative of spring flow and potential salamander habitat are dependent upon the length of time in which the area is consistently dominated by the groundwater flow. The floods appear to remove the spring-associated vegetation but regrowth occurs when baseflow conditions re-establish previous flow regimes.

Springs Assessment

SIP/SEAP

Salado Springs is recognized locally as an important natural resource, cultural landmark, and ecosystem that needs thoughtful and sustainable management. While springs are often considered as important and sensitive ecosystems, researchers recognize that a consistent language to describe and classify springs is lacking. Stevens and others (2011) propose a set of protocols for the holistic inventory and monitoring of springs. The objective of a consistent language and classification system for springs is to facilitate consistent guidelines for the conversation, management, restoration, and research of spring ecosystems. The classification system described by Stevens and others (2011) was applied to Salado Springs as a summation of the hydrogeological knowledge that has been collected at the springs through this body of research. Using terminology that is consistent with other spring researchers may allow researchers and managers of Salado Springs to better compare Salado Springs to other spring systems.

The classification process developed by Stevens and others aims to integrate pre-existing spring classification systems into a methodology that can be consistently applied to different spring ecosystems at differing levels of effort. The process involves two steps: The first step is an integrated *springs inventory protocol* (SIP) to quickly and reliably provide information on spring ecosystem components, processes, threats, and stewardship options (Stevens and others, 2011). Results from the SIP may be uploaded to an online database for comparison with other springs at the national and international levels. Furthermore, SIP results feed into a comprehensive secondary assessment, the *springs ecosystem assessment protocol* (SEAP). SEAP facilitates comparison of springs within a landscape, determination of stewardship priorities, monitoring, and measurement of the effectiveness of management actions (Stevens and others, 2011). Data sheets for both the SIP and SEAP are included in Appendix B for reference.

As part of the SIP and SEAP, springs of interest are classified into 12 spring types. Each spring type is described as a “sphere of discharge”, which is the idea that springs may be distinguished from each other by the environmental setting, or “sphere”, into which groundwater is discharged (Springer and others, 2008). The 12 spheres of discharge of springs originally described by Springer and others (2008) and further explained by Springer and Stevens (2009) are: Cave springs, exposure springs, fountain springs, geyser springs, gushet springs, hanging garden springs, helocrene springs, hillslope springs, hypocrene springs, limnocrene springs, mound-form springs, and rheocrene springs. In the Salado Springs complex, springs may be classified as rheocrene springs or limnocrene springs; characteristics of certain springs fit into and be classified as a combination of spring types.

A rheocrene spring (Figure 28) is defined as a flowing spring that emerges into one or more stream channels, or “spring runs”. The relatively uniform temperature and de-oxygenated groundwater in a spring run can create unique habitat conditions. Hydrogeochemical stability of a spring run is modified by groundwater interaction with surface water or runoff, disturbance frequency, and geomorphology (Springer and others, 2008); these factors influence the microhabitats that exist in a rheocrene spring setting, which in turn may support specialist aquatic species and evolutionary adaptation (in groundwater-dominated spring runs) or generalist, weedy species (surface water-dominated spring runs (Griffiths and others, 2008; McCabe, 1998). In Salado, parts of groundwater-dominated spring runs are habitat for the Salado salamander (*Eurycea chisolmensis*).

A limnocrene spring (Figure 29) is defined as a groundwater that is discharged from a confined or unconfined aquifer into one or more lentic, or still-water, pools. Limnocrene springs may be inhabited by pond and aquatic species, but their relatively uniform temperature and chemistry may support different species than those that are present in an adjacent surface water-dominated water body (Springer and Stevens, 2009).

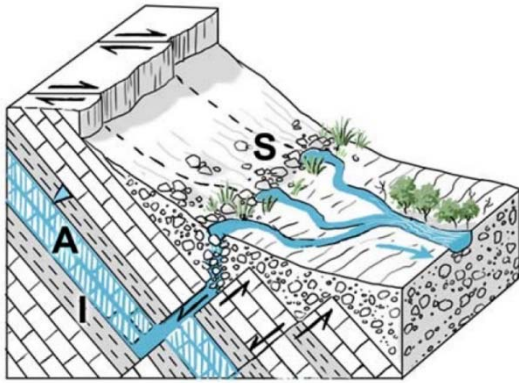


Figure 28. Rheocrene spring (Springer and Stevens, 2009). In the spring diagrams, A represents the aquifer, I is impermeable stratum, S is the spring source, and the inverted triangle represents the water table.

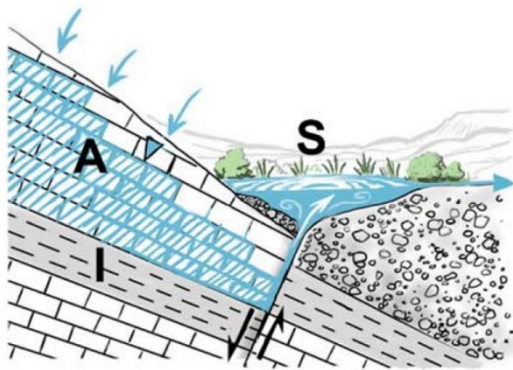


Figure 29. Limnocrene spring (Springer and Stevens, 2009). In the spring diagrams, A represents the aquifer, I is impermeable stratum, S is the spring source, and the inverted triangle represents the water table.

Solar budget (Solar Pathfinder™)

One aspect of the SIP assessment is performing a solar budget evaluation for each spring site. Knowing the amount of exposure a spring site has to the sun can be important for understanding the ecology of the spring, including temperature dynamics and what types of plants and animals can thrive. Using a Solar Pathfinder™ (SPF; The SolarPathfinder Company, Linden, Tennessee), the shading pattern across a given site is determined (Figure 30, left). A highly polished, transparent, convex dome gives a panoramic view of the entire site and shows tall plants or rock outcrops that can potentially shade a spring site. The edge of possible shade-structures are traced onto latitude-specific sunpath diagrams, specialized charts with rays that show solar time and arcs that show months of the year (Figure 30, right). By combining the tracing with the sunpath diagram, researchers can determine when a spring site will be shaded during the year. A SPF evaluation was performed for each spring in the Salado Springs complex on September 22, 2016 and the sunpath diagrams are documented in Appendix C. Results from SPF evaluations are entered into the “SPF” field of the SIP datasheet as part of the overall spring assessment.

SIP Results and Recommendation

In 2016, springs in the Salado Springs complex, Robertson Spring as well as all the major downtown springs, were categorized according to their spheres of discharge. Robertson Spring is comprised of multiple orifices, some which discharge into spring runs, and others that discharge from the floor of a stream or spring run; Robertson Spring is best described as both a rheocrene spring and a limnocrene spring (Figure 31). At Big Boiling Spring, groundwater discharges from one major ground-level orifice at the head of a large spring run and pool; because of these characteristics, Big Boiling Spring is best described as both a rheocrene spring and a limnocrene spring (Figure 32). Little Bubbly spring, which discharges into a spring run (61 ft) that flows into the pool of Big Boiling Spring, is best described as a rheocrene spring (Figure 33). Side Spring is also described as a rheocrene spring because groundwater discharges into a short spring run (11 ft) that flows into Salado Creek (Figure 34). Critchfield Spring discharges from a ground-level orifice that forms a groundwater pool. Water flows out of the northern end of the

pool to feed a spring run that flows parallel to Salado Creek for about 250 ft before flowing into the Doc Benedict Spring pool. Critchfield Spring is best described as both a limnocene spring and a rheocene spring (Figure 35), while Doc Benedict Spring is best described as a limnocene spring (Figure 36). Lastly, Anderson Spring, which also discharges from a ground-level orifice, is best described as a limnocene spring (Figure 37).

The SIP process was initiated in 2016. However, more time and study are necessary to develop a reasonably complete SIP document for each of the springs. It is recommended that the SIP process continue until the files are more complete and then the results presented in a separate report to the CUWCD board for approval.

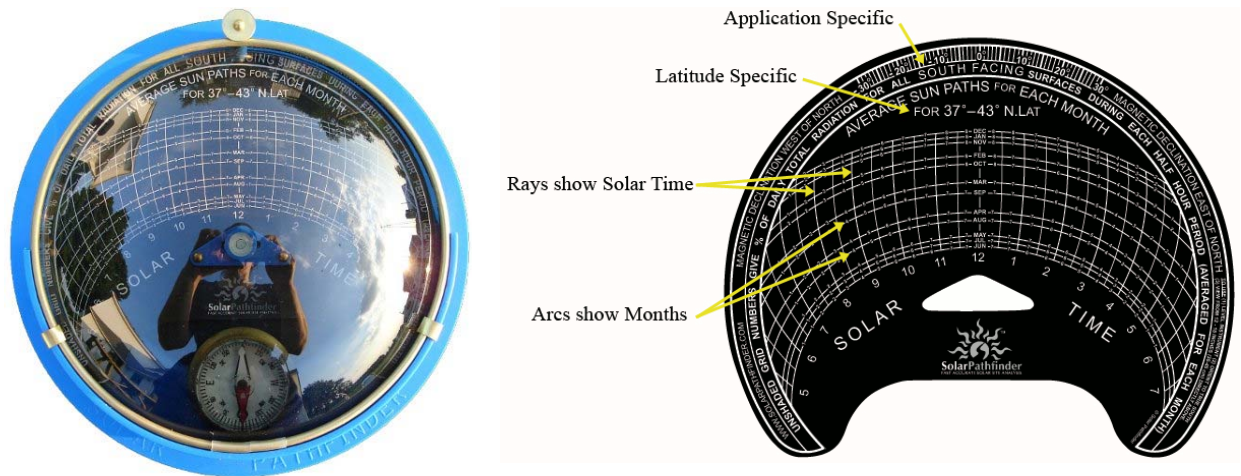


Figure 30. The Solar Pathfinder™. *Left*, a transparent dome gives a panoramic view around a site, showing surrounding shade structures. *Right*, an example sunpath diagram. (Images from Solar Pathfinder™, 2017).



Figure 31. Robertson Spring has characteristics of both a rheocene spring (*left*) as well as a limnocene spring (*right*). Location of the Solar Pathfinder™ is indicated by the crossed circle (⊕) in the *left* photo.



Figure 32. Big Boiling Spring has characteristics of a rheocrene spring and a limnocrene spring. Location of the Solar Pathfinder™ is indicated by the crossed circle (⊕).



Figure 33. Little Bubbly Spring is best classified as a rheocrene spring. Location of the Solar Pathfinder™ is indicated by the crossed circle (⊕).



Figure 34. Side Spring is best classified as a rheocrene spring. Location of the Solar Pathfinder™ is indicated by the crossed circle (⊕). The photo on the *right* shows Stephanie Wong working with the Solar Path Finder at Side Spring.



Figure 35. Critchfield Spring has characteristics of both a limnocrene spring as indicated by the pool on the *left*, as well as a rheocrene spring as indicated by the spring run on the *right*. Location of the Solar Pathfinder™ is indicated by the crossed circle (⊕) in the photo on the *left*.



Figure 36. Doc Benedict Spring is best classified as a limnocrene spring. Location of the Solar Pathfinder™ is indicated by the crossed circle (⊕).

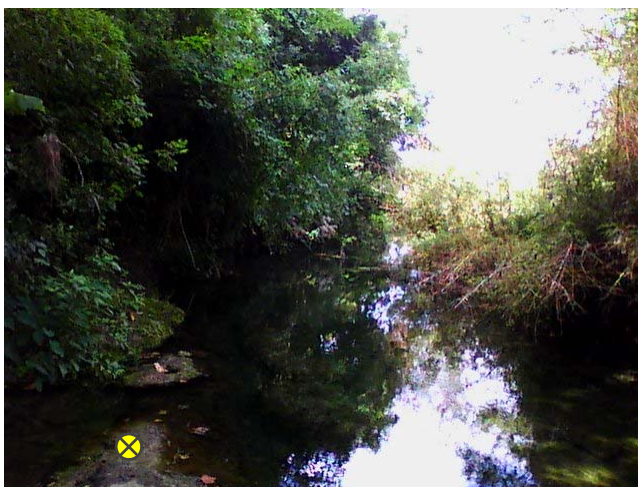


Figure 37. Anderson Spring is best classified as a limnocrene spring. Location of the Solar Pathfinder™ is indicated by the crossed circle (⊕).

Summary and Project Conclusions

The continuation of research on the Northern Segment has produced new data and new insights into the groundwater flow dynamics of the Northern Segment of the Edwards Balcones Fault Zone aquifer, particularly the downtown Salado Springs complex. Findings are summarized below.

1. Using LiDAR data to detect recharge features still looks promising for determining areas of important recharge potential. Several depressions in the Robertson ranch were detected and an aspect map identified lineations which parallel faults/fractures associated with the springs and warrant further analysis. However, the efforts to this point indicate an analysis of temporal and spatial rainfall patterns coupled with the Cave Well hydrographs may be more insightful in delineating important areas of recharge.
2. Data collected with a multi-parameter datalogger in the Stagecoach Inn Cave well indicated rapid groundwater responses to large rainfall events. The data also show slight water quality changes. The responses to recharge captured by the datalogger provides important timing information to aid in the development of future monitoring strategies.
 - a. Nitrogen data from field and laboratory analysis showed values that are interpreted to be slightly above expected background levels but no nitrate values were observed to be over the drinking water limit.
 - b. The nitrogen data warrant further investigation and monitoring.
3. Data collected with a Solinst hand-held meter along cross-sections of Salado Creek and adjacent springs show patterns helpful in understanding groundwater/surface-water interactions and potential areas of salamander habitat.
 - a. Specific conductance (SC) and temperature (T) measurements in cross sections of Big Boiling Spring as well as upstream and downstream of the confluence between Big Boiling Spring discharge and Salado Creek confirm the mixing patterns of groundwater and surface water from Big Boiling Spring.
 - b. The cross section data are important to quantify groundwater/surface water mixing, aid in habitat assessments, and aid in sample location selection.
 - c. The groundwater from Big Boiling Spring appears to mimic laminar flow and hug the south bank of Salado Creek for tens of yards before structural features in the stream enable mixing with the surface water of the creek. The groundwater influence is dependent upon the ratio of the flow between the creek and the spring.
4. Thermography using a handheld FLIR camera has helped delineate potential salamander habitat in the springs and spring runs at several springs. The thermography also has better delineated the exact areas of groundwater interaction with surface water and confirmed previous cross section studies.
5. Spring Inventory protocol (SIP) and Spring Ecosystem Assessment Protocol (SEAP) were used to categorize the springs in the downtown area with internationally published protocols for comparisons of baseline and possibly future management conditions.

Recommendations

Recharge feature characterization

While providing new insights on methods for characterizing the aquifer, the large data volume and time required to perform Lidar data analysis is not efficient for aquifer-wide analysis in general. A more efficient work-flow may be to examine spatial distribution of precipitation and pair these data with hydrograph analysis to determine important recharge areas, then perform a second-level examination of the area using Lidar data to identify recharge features.

Groundwater monitoring

Aquifer conditions

The OTT CTD datalogger is a reliable instrument that provides consistent data and requires minimal maintenance; recommended that CUWCD continue monitoring at the SCI Cave well with this instrument. There is a need to determine a fixed benchmark in the cave to tie all water level measurements to through time. Maintenance once every 4-6 months is recommended, including replacement of desiccant tablets and recalibration of specific conductance sensor. Visits to the site are recommended once every month. This is necessary to download data, check battery power, and observe site conditions.

Nitrate

Calibration and maintenance of the In-Situ Troll 9500 instrument has been an involved process. Magnitude of nitrate concentrations from the In-Situ Troll 9500 do not compare well with results from lab analysis. Therefore, we recommend monitoring the long-term nitrate trend through periodic (annual or semi-annual) grab samples at key springs and monitoring wells.

Groundwater – surface water interaction

The FLIR infrared camera and profiling of spring discharge using temperature, specific conductance, and flow produced some useful insights into groundwater and surface water interactions. This technique may be useful at other spring locations within the Salado Creek Basin.

Springs assessment

While the spring assessment process has been started, more time and study are necessary to develop a reasonably complete SIP document for each of the springs. It is recommended that the SIP process continue until the files are more complete and then the results presented in a separate report to the CUWCD board for approval.

References

- Blackwell, P.R., and G. Wells, 1999, DEM resolution and improved surface representation. *In* ESRI Users Conference, Proceedings, June 1999.
- ESRI, 2017a, Hydrology toolset concepts: How Fill works *in* Tool Reference. <<http://pro.arcgis.com/en/pro-app/tool-reference/spatial-analyst/how-fill-works.htm>> *Last accessed 12 April 2017.*
- ESRI, 2017b, Surface toolset concepts: How Aspect works *in* Tool Reference. <<http://desktop.arcgis.com/en/arcmap/10.3/tools/spatial-analyst-toolbox/how-aspect-works.htm>> *Last accessed 13 April 2017.*
- Griffiths, R.E., A.E. Springer, and D.E. Anderson, 2008, The morphology and hydrology of small spring-dominated channels. *Geomorphology*, 102(3-4): 511-521.
- Gritzner, J.H., 2006, Identifying wetland depressions in bare-ground LIDAR for hydrologic modeling. *In* Proceedings of the twenty-sixth annual ESRI user conference, July 2006. 13 pp.
- Jones, I.C., 2003, Groundwater Availability Modeling: Northern Segment of the Edwards Aquifer. Texas Water Development Board Report 358, Austin, Texas, 75 pp.
- Kreitler, C.W., and L.A. Browning, 1983, Nitrogen-isotope analysis of groundwater nitrate in carbonate aquifer: Natural sources versus human pollution. *Journal of Hydrology*, 61:285-301.
- McCabe, D.J., 1998, Biological communities in springbrooks. *In* Studies in Crenobiology: The biology of springs and springbrooks, Botosaneanu, L. (Ed.). Backhuys, Leiden, The Netherlands.
- Slade Jr., R.M., M.E. Dorsey, and S.L. Stewart, 1986, Hydrology and water quality of the Edwards Aquifer associated with Barton Springs in the Austin area, Texas. U.S. Geological Survey Water Resources Investigations Report 86-4036, Austin, Texas, 123 pp.
- Solar Pathfinder™, 2017, Solar Pathfinder™ website. <<http://www.solarpathfinder.com/PF?id=TaBkNLSW#sunpath>> *Last accessed 27 July, 2017.*
- SonTek. 2007. FlowTracker® Handheld ADV® Technical Manual. SonTek/YSI Inc., San Diego, CA. 126 pp.
- Sorman, A.U., and M.J. Abdulrazzak, 1993, Infiltration-recharge through wadi beds in arid regions. *Hydrological Sciences Journal*, 38(3): 173-186.
- Springer, A.E., and L.E. Stevens, 2009, Spheres of discharge of springs. *Hydrogeology Journal*, 17:83-93. DOI 10.1007/s10040-008-0341-y
- Springer, A.E., L.E. Stevens, D.E. Anderson, R.A. Parnell, D.K. Kreamer, L. Levin, and S. Flora, 2008, A comprehensive springs classification system: integrating geomorphic, hydrogeochemical, and ecological criteria. *In* Aridland springs in North America: ecology and conservation, Stevens, L.E. and V.J. Meretsky (Eds.). University of Arizona Press, Tucson, Arizona.
- Springs Stewardship Institute, 2014, SIP and SEAP Field Sheets. <<http://docs.springstewardship.org/PDF/FieldFormOct2014.pdf>> *Last accessed 7 December, 2016.*
- Stevens, L.E., A.E. Springer, J.D. Ledbetter, 2011, Inventory and monitoring protocols for springs ecosystems, Version: 1 June 2011. 64 pp. <http://docs.springstewardship.org/PDF/Springs_Inventory_Protocols_110602.pdf> *Last accessed 7 December 2016.*
- Texas Natural Resources Information System (TNRIS), 2017, StratMap2011 50cm Bell, Burnet, McLennan. <<https://tnris.org/data-catalog/entry/stratmap-2011-50cm-bell-burnet-mclennan/>> *Last accessed 13 April 2017.*
- Turnipseed, D.P., and V.B. Sauer, 2010, Discharge measurements at gaging stations: U.S. Geological Survey Techniques and Methods book 3, chap. A8, 87p.
- Zhang, Y.K., and K.E. Schilling, 2006, Effects of land cover on water table, soil moisture, evapotranspiration, and groundwater recharge: A field observation and analysis. *Journal of Hydrology*, 319(1-4): 328-338.

Appendix A
Dissolved nitrate/nitrite concentrations for Salado Springs

Table A1. Dissolved nitrate/nitrite content in groundwater and surface water at Salado Springs on February 11-16, 2016 (low-traffic weekend). Concentrations are reported in mg/L.

Site	Pre-weekend	Weekend	Post-weekend
Main Street Bridge (<i>upstream</i>)	2.84	2.70	2.70
Stagecoach Inn Cave Well	4.09	4.10	4.26
Big Boiling Spring	4.31	4.28	4.25
Little Bubbly Spring	4.07	4.25	4.14
Side Spring	4.25	4.27	4.21
Critchfield Spring	4.05	3.87	4.07
Doc Benedict Spring	3.82	3.65	3.75
Anderson Spring	4.09	4.00	3.81
Inn on the Creek (<i>downstream</i>)	3.12	3.04	3.07

Table A2. Dissolved nitrate/nitrite content in groundwater and surface water at Salado Springs on March 23-30, 2016 (Easter long-weekend). Concentrations are reported in mg/L.

Site	Pre-weekend	Weekend	Post-weekend
Main Street Bridge (<i>upstream</i>)	1.73	1.4	1.27
Stagecoach Inn Cave Well	2.87	2.44	2.92
Big Boiling Spring	2.87	2.76	2.69
Little Bubbly Spring	2.91	3.02	2.81
Side Spring	2.78	3.04	2.87
Critchfield Spring	3.21	2.73	2.84
Doc Benedict Spring	2.38	2.38	2.43
Anderson Spring	2.62	2.38	2.52
Inn on the Creek (<i>downstream</i>)	1.69	1.66	1.60

Table A3. Dissolved nitrate/nitrite content in groundwater and surface water at Salado Springs on September 1-7, 2016 (Labor Day long-weekend). Concentrations are reported in mg/L.

Site	Pre-weekend	Weekend	Post-weekend
Main Street Bridge (<i>upstream</i>)	1.62	1.41	1.68
Stagecoach Inn Cave Well	2.40	3.31	1.88
Big Boiling Spring	2.48	2.68	3.31
Little Bubbly Spring	3.11	3.77	3.84
Side Spring	2.66	3.02	2.85
Critchfield Spring	3.65	2.38	3.43
Doc Benedict Spring	2.58	3.41	3.09
Anderson Spring	2.89	3.44	2.64
Inn on the Creek (<i>downstream</i>)	2.00	1.72	2.28

Table A4. Dissolved nitrate/nitrite content in groundwater and surface water at Salado Springs on September 14-21, 2016 (Salado Chocolate and Wine event-weekend). Concentrations are reported in mg/L. Several samples were collected but not analyzed due to an error in sample identification. Unanalyzed samples are denoted by N/A.

Site	Pre-weekend	Weekend	Post-weekend
Main Street Bridge (<i>upstream</i>)	1.54	N/A	2.37
Stagecoach Inn Cave Well	N/A	N/A	3.67
Big Boiling Spring	3.57	N/A	3.69
Little Bubbly Spring	2.61	N/A	3.68
Side Spring	3.02	N/A	3.69
Critchfield Spring	3.72	N/A	3.67
Doc Benedict Spring	3.45	2.71	3.53
Anderson Spring	N/A	N/A	3.59
Inn on the Creek (<i>downstream</i>)	2.05	2.4	2.73

Appendix B
Spring Assessment: SIP and SEAP datasheets
(Springs Stewardship Institute, 2014)

1 Discharge Sphere (Spring Type)

Anthropogenic
 Cave
 Exposure
 Fountain
 Geyser
 Gushet
 Hanging Garden
 Helocrene
 Hillslope
 Hypocrene
 Limnocrene
 Mound-form
 Rheocrene

2 Sensitivity

None
 Location
 Survey
 Both

3 Land Unit

BLM
 DOE
 NPS
 Private
 State
 Tribal
 USFS
 Other

4 Georeference Source

GPS
 Map
 Other

5 Surface Type

BW Backwall
 C Cave
 CH Channel
 CS Colluvial slope
 HGC High Grad. Cienega
 LGC Low Grad Cienega
 Mad Unfocused Madiculous
 O Organic Ooze
 P Pool
 PP Plunge Pool
 SB Sloping Bedrock
 SM Spring Mound
 TE Terrace
 TU Tunnel
 Upl Adjacent Uplands
 WH Wet Hillslope
 Oth Other

6 Surface Subtype

CH Riffle, Run, Margin, Eph
 TE LRZ, MRZ, URZ, HRZ
 UPL,LRZMRZ,LRZURZ,
 MRZURZ, HRZMRZ
 All Anthro

7 Slope Variability

Low, Medium, High

8 Soil Moisture

1 - Dry
 2 - Dry-Moist
 3 - Moist-Dry
 4 - Wet-Dry
 5 - Moist
 6 - Saturated-Dry
 7 - Wet
 8 - Saturated-Moist
 9 - Wet-Saturated
 10 - Saturated
 11 - Inundated

9 Substrate

1 clay
 2 silt
 3 sand
 4 fine gravel
 5 coarse gravel
 6 cobble
 7 boulder
 8 bedrock
 Organic Soil/Matter
 Other/anthropogenic

10 Lifestage

Adult
 Egg
 Exuvia
 Immature
 Larvae
 Mixed
 Other
 Pupae
 Shell

11 Habitat

AQ - Aquatic
 T - Terrestrial

12 Method (Invertebrates)

Spot
 Benthic

13 Detection Type (Vertebrates)

Call
 Observed
 Sign
 Reported (by others)
 Other

14 Cover Codes

GC Ground Cover
 SC Shrub Cover
 MC Midcanopy Cover
 TC Tall Canopy Cover
 AQ Aquatic Cover
 NV Nonvascular (moss, etc)
 BC Basal Cover

15 Emergence Environ/Detail

Cave
 Subaerial
 Subglacial
 Subaqueous-lentic freshwater

Subaqueous-lotic freshwater
 Subaqueous-estuarine
 Subaqueous-marine

16 Source Geomorphology

Contact Spring
 Fracture Spring
 Seepage or filtration
 Tubular Spring

17 Flow Force Mechanism

Anthropogenic
 Artesian
 Geothermal
 Gravity
 Other

18/19 Parent Rock Type/Subtype

Igneous
 andesite
 basalt
 dacite
 diorite
 gabbro
 grandodiorite
 granite
 peridotite
 rhyolite
 Metamorphic
 gneiss
 marble
 quartzite
 slate
 schist
 Sedimentary
 coal
 conglomerate
 dolomite
 evaporates
 limestone
 mudstone
 sandstone
 shale
 siltstone
 Unconsolidated

20 Channel Dynamics

Mixed runoff/spring dominated
 Runoff dominated
 Spring dominated
 Subaqueous

21 Flow Consistency

Dry intermittent
 Erratic intermittent
 Perennial
 Regular intermittent

22 Measurement Technique

Current meter
 Weir
 Cutthroat flume
 Other

©Springs Stewardship Institute rev 10/14

Spring Name _____ Page _____ of _____ OBS _____

Invertebrates	Species Name	Qty	¹⁰ Stage	¹¹ Habitat	¹² Method	Rep #	Comments	
Benthic Rep	Rep #	Location	Velocity m/sec	Depth cm	Substrate	Area Sq M	Time Sec	Comments

Entered by _____ Date _____ Checked by _____ Date _____

Aquifer/WQ	Cond	Risk	Habitat	Cond	Risk	Human Influence	Cond	Risk	Administrative Context	Cond	Risk
Spring dewatered (Y/N)			Isolation			Surface water quality			Information quality/quantity		
Aquifer functionality			Habitat patch size			Flow regulation			Cultural significance		
Spring discharge			Microhabitat quality			Road/trail/railroad			Historical significance		
Flow naturalness			Native plant ecological role			Fencing			Recreational significance		
Flow persistence			Trophic dynamics			Construction			Economic value		
Water quality			Score			Herbivory			Conformance to mgmt plan		
Algal and periphyton cover			Biotic Integrity			Recreational			Scientific/educational value		
			Native plant richness/diversity			Adjacent conditions			Environmental compliance		
Geomorphology			Native faunal diversity			Fire influence			Legal status		
Site obliterated (Y/N)			Sensitive plant richness								
Geomorphic functionality			Sensitive faunal richness								
Runout channel Geometry			Nonnative plant rarity								
Soil integrity			Nonnative faunal rarity								
Geomorphic diversity			Native plant demography								
Natural physical disturbance			Native faunal demography								

Notes:

Recommendations:



Appendix C
Sunpath diagrams for Salado Springs

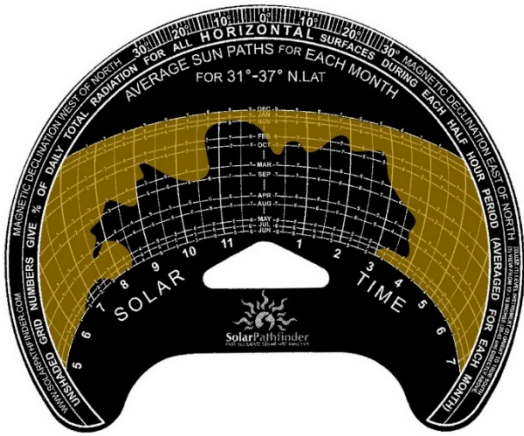


Figure C-1. Sun path diagram for Robertson (Ludwigia) Spring, October 27, 2016.

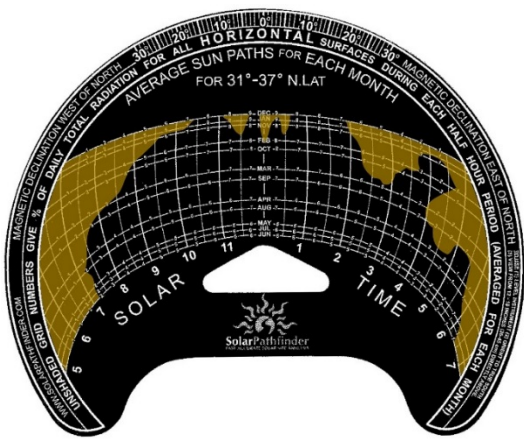


Figure C-2. Sun path diagram for Big Boiling Spring, September 22, 2016.

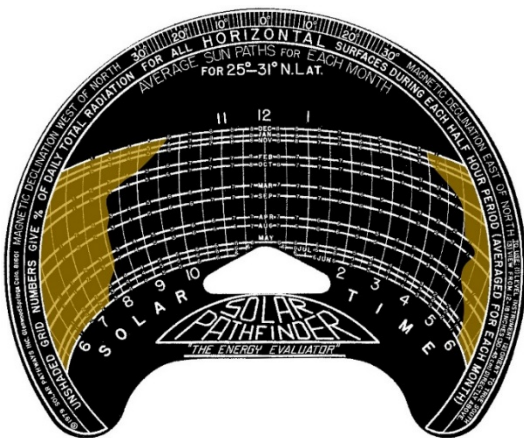


Figure C-3. Sun path diagram for Little Bubbly Spring, September 22, 2016.

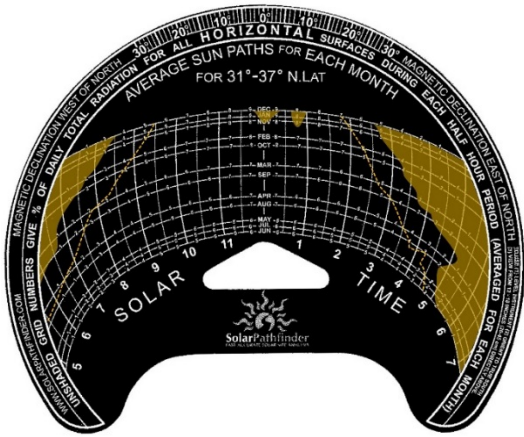


Figure C-4. Sun path diagram for Side Spring, September 22, 2016.

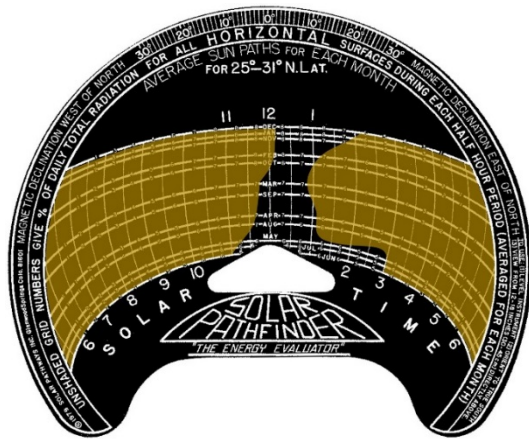


Figure C-5. Sun path diagram for Critchfield Spring, September 22, 2016.

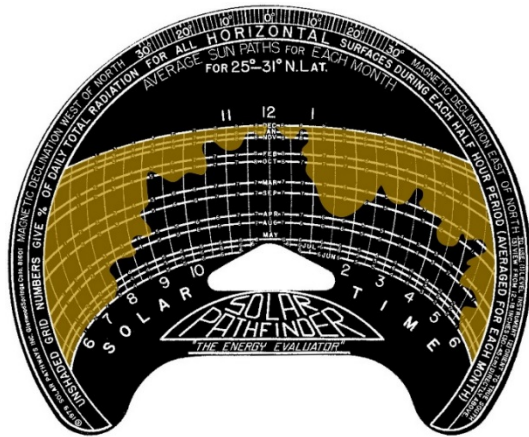


Figure C-6. Sun path diagram for Doc Benedict Spring, September 22, 2016.

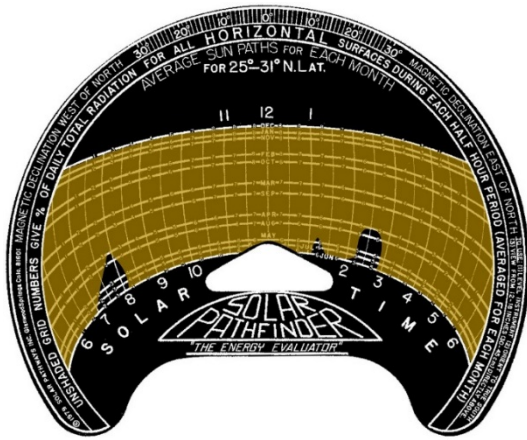


Figure C-7. Sun path diagram for Anderson Spring, September 22, 2016.